Megascopic processes reflected in the microscopic realm

sedimentary and biotic dynamics of the Middle Ordovician “orthoceratite limestone” at Kinnekulle, Sweden

Lindskog, Anders; Eriksson, Mats E.

Published in:
GFF

DOI:
10.1080/11035897.2017.1291538

2017

"This is the peer reviewed version of the following article: Lindskog, A. & Eriksson, M.E. 2017. Megascopic processes reflected in the microscopic realm: sedimentary and biotic dynamics of the Middle Ordovician 'orthoceratite limestone' at Kinnekulle, Sweden. GFF 139, 163-183., which has been published in final form at https://doi.org/10.1080/11035897.2017.1291538."

Megascopic processes reflected in the microscopic realm: sedimentary and biotic dynamics of the Middle Ordovician 'orthoceratite limestone' at Kinnekulle, Sweden

Anders Lindskog[1,*] & Mats E. Eriksson[1]
[1] Department of Geology, Lund University, Sölvegatan 12, SE-223 62 Lund, Sweden; anders.lindskog@geol.lu.se, mats.eriksson@geol.lu.se
[*] Corresponding author

ABSTRACT
The Middle Ordovician (Dapingian–middle Darriwilian) 'orthoceratite limestone' is documented in its traditional type area at Kinnekulle in the province of Västergötland in southern Sweden. Detailed field studies combined with systematic qualitative and quantitative analyses of carbonate microfacies at high stratigraphic resolution show that this suite of cool-water carbonate rocks is more variable than is suggested by its overall homogeneous macroscopic appearance. Long-term changes in carbonate textures and fossil grain assemblages, together with pervasive rhythmic/cyclic patterns, suggest a strong influence from sea level on microfacies characteristics. Assessment of the results in light of regional facies patterns indicates that the cool-water 'orthoceratite limestone' behaved much like 'model' siliciclastic sedimentary systems, in that carbonate texture varied with depositional depth as particle size of siliclastics does. Carbonate texture thus appears to reflect absolute depth well, whereas grain assemblages record high-frequency cycles of changes in both sea level and substrate conditions. A relative sea level curve compiled from the collective data shows excellent agreement with previously published curves based on different proxies. The most important factor for the long-term establishment and regional dominance of the 'orthoceratite limestone' throughout much of the Early and Middle Ordovician appears to have been a limited terrigenous sediment input to the Baltoscandian paleobasin. Hence, much of the regional facies zonation may reflect distance from weathering sources rather than water depth.

Keywords: Carbonate sedimentology; microfacies; paleoecology; cool-water carbonates; sea level; lower Paleozoic

Introduction

The Ordovician was a time of record-high global sea level and, consequently, epeiric seas covered large parts of the paleocontinents. These extensive shallow-water areas were the scenes of remarkable changes within the global marine biota during the so-called Great Ordovician Biodiversification Event (GOBE), which brought along numerous new taxa and the establishment of new ecologic niches (e.g., Webby et al. 2004; Servais et al. 2009; Algeo et al. 2016). In recent years, the overall view of the Ordovician Period has changed drastically from an exotic 'Greenhouse world' into one with a climate more akin to that of today (e.g., Trotter et al. 2008; Pohl et al. 2016; Rasmussen et al. 2016) yet many details remain enigmatic and even contradictory; sedimentary rocks and their entombed fossils form the archive from which information about the paleoenvironment is extracted, but a lack of modern analogues to the vast epeiric seas and their extinct biota compounds interpretations (e.g., Rutten 1949). A better understanding of the links between the sedimentary and biotic development is key to revealing more information about the past.

In Sweden, large parts of the Lower to Middle Ordovician are represented by a condensed succession of cool-water carbonates informally named the 'orthoceratite limestone' (e.g., Lindström 1971a; Jaanusson 1973, 1982a). These rocks are typically described as being homogeneously developed across both space and time, as they show only limited variability at the macroscopic scale

(e.g., Lindström 1963; Olgun 1987). The relatively low-diversity fossil macrofauna found within the 'orthoceratite limestone' holds few and often ambiguous clues about the depositional environment and the macroscopic homogeneity of the rock is of little help. Hence, as is the case for carbonates in general, analyses of composition, fabrics and textures at the microscopic scale – i.e. microfacies – are of essential importance in the characterization of the 'orthoceratite limestone'. Some detailed analyses have been undertaken over the years (e.g., Hadding 1958; Jaanusson 1972; Olgun 1987), but the data have seen little use beyond descriptive aims and the depositional system in which the 'orthoceratite limestone' formed has remained poorly understood.

This study documents the macroscopic and microscopic characteristics of the Middle Ordovician 'orthoceratite limestone' in its type area at Kinnekulle in southern Sweden. Detailed field studies are combined with systematic carbonate microfacies analyses, in a holistic approach to extract information about the paleoenvironmental development at several spatiotemporal scales. The central location of Kinnekulle within the Baltoscandian paleobasin, together with its relatively thick sedimentary succession, offers ideal conditions to resolve previous contradictory interpretations between proximal and distal areas. The results provide insight into the behavior of ancient epeiric seas and cool-water carbonate depositional systems in particular, and show that microfacies variations can record larger-scale environmental events.

Geologic setting

During much of the early Paleozoic, large parts of northwestern Europe lay submerged by epeiric seas. The preserved remnants of a thin blanket of sedimentary deposits throughout Sweden and its geographic surroundings record a long-term transgression that begun already in the late Precambrian and led to a near-complete marine covering of the Baltoscandian region during the Ordovician (Fig. 1). Landmasses largely consisted of peneplanes with insignificant relief, which limited export of terrigenous weathering products, and net sedimentation rates in the paleobasin typically reached only a few millimeters per millennium. Following a dominance of siliciclastic sedimentation in the Cambrian and early Ordovician, most of the Ordovician was characterized by a widespread deposition of carbonates (e.g., Lindström 1971a). In the Middle Ordovician, the 'orthoceratite limestone', a condensed cool-water carbonate facies, forms the main rock in Sweden. It was originally deposited across large areas of the country, but today only patches occur where conditions have provided shelter from subsequent erosion. This rock, which comes in a variety of gray and reddish brown hues, has seen much use for building purposes and stonemasonry. The 'orthoceratite limestone' is typified by a variable mixture of calcareous mud and sand-sized skeletal grains with only limited terrigenous matter. Fossil abundance varies markedly and the biodiversity typically is relatively low. Outcrops show little variation at the macroscopic scale and few signs of tectonic disturbance (e.g., Lindström 1979; Jaanusson 1973, 1982a).

The province of Västergötland in south-central Sweden hosts several exposures of the 'orthoceratite limestone', which occurs within a set of isolated hills traditionally referred to as table mountains. These mountains were preserved largely due the intrusion of dolerite sills during the Permian that later acted as protective caps (e.g., Munthe 1905; Priem et al. 1968). The Paleozoic succession of Västergötland has a long study tradition that reaches back to the 1700s, and a chronicle of early geologic investigations in Västergötland can be found in Moberg (1910). On the southeastern shore of Lake Vänern, the c. 300-m-high table mountain Kinnekulle forms a Paleozoic 'island', clearly shaped by large-scale glacial processes in the relatively recent past, on top of the peneplaned Precambrian bedrock that otherwise characterizes this area (Fig. 2; Holm & Munthe 1901; Högbom & Ahlström 1924; Westergård 1943; Gillberg 1970). The sedimentary succession of Kinnekulle spans the Cambrian Series 2 through the Llandovery Series of the Silurian, and the latter terminates upward against dolerite (Fig. 3). Kinnekulle has been designated as the type area for the 'orthoceratite limestone' (Hisinger 1828; Jaanusson 1982b).

The interval studied here spans the uppermost Floian through middle Darriwilian of the Lower–Middle Ordovician (see Bergström et al. 2009). The basal part of the studied succession comprises the uppermost Tøyen Shale, spanning the transition between the Billingen and Volkhov Baltoscandian stages (uppermost Fl3). The Lanna limestone follows above, and is in turn overlain by the Holen limestone. The Tøyen–Lanna boundary closely coincides with that between the Floian and Dapingian

global stages (e.g., Bergström & Löfgren 2009; Lindskog 2014). The Lanna–Holen limestone interval, colloquially known as the 'Rödsten' ('Redstone'; Holm 1901) due to the characteristic reddish brown color, constitutes the 'orthoceratite limestone' proper and is the main target of this study. The Lanna and Holen limestones belong to the topostratigraphic framework developed by Jaanusson (1960, 1976, 1982a–c), which combines lithologic and paleontologic criteria in the subdivision of strata. Hence, although the Lanna and Holen limestones have come to wide use in the scientific literature, they remain informal topoformations (see below). In their regular use, the Lanna and Holen limestones roughly represent the Volkhov (uppermost Fl3–lowermost Dw1) and Kunda (Dw1–upper Dw2) Baltoscandian stages, respectively (e.g., Lindskog et al. 2014). A conspicuous c. 1.5-m-thick gray limestone interval occurs in the lower Holen limestone across Kinnekulle. These gray beds are referred to as the 'Täljsten' ('Carving stone', i.e., practically quarriable rock suitable for stonemasonry). The 'Täljsten' has long been known for its peculiar facies and paleontologic characteristics, perhaps best exemplified by the presence of beds abounding with *Sphaeronites* cystoids (see Linnarsson 1866, 1869; Holm 1901; Eriksson et al. 2012). At Kinnekulle, the top of the Holen limestone is drawn at a discontinuity surface that marks an extensive hiatus encompassing the entire Aseri Baltoscandian Stage and most of the succeeding Lasnamägi Stage (Jaanusson 1964; Holmer 1983; Zhang 1998a). The Holen limestone is thus disconformably overlain by the thin Skövde limestone (Lasnamägi, middle Dw3). The Gullhögen Formation (Uhaku, upper Dw3; e.g., Zhang 1998b), the basal beds of which form the top of the studied succession, follows above. The Skövde and Gullhögen beds, together with the overlying Ryd limestone (Uhaku), have traditionally been referred to as the 'Leversten' ('Liverstone'). The top of the Holen limestone coincides with the boundary between the Öland and Viru Baltoscandian series, which in older literature is cited as the (obsolete) regional Lower–Middle Ordovician boundary (e.g., Jaanusson 1964, 1982a). A guide for geologic nomenclature was recently introduced for the country of Sweden (Kumpulainen 2017). The guidelines (rightfully) deem topostratigraphy obsolete, thus necessitating the replacement of topostratigraphic units with formally ratified formations. However, as the stratigraphic framework of the interval studied herein has not been formally reviewed and further work clearly is needed for this to be done, the present study retains the topostratigraphic nomenclature. Formations outside of the topostratigraphic tradition, that are generally recognized and treated as lithoformations, are provisionally treated as formal units.

The 'Rödsten' at Kinnekulle has been extensively quarried and a string of abandoned quarries now trace the distribution of the 'orthoceratite limestone' around the table mountain (Fig. 2). Most quarries were centered around the 'Täljsten', as this level is easily recognizable and of reliable quality. Only the northernmost part of the table mountain, which hosts a relatively deep soil cover, has escaped quarrying activities (e.g., Johansson et al. 1943). Today, only the Såtaskogen and Thorsberg quarries remain active. The latter has become known for the numerous fossil meteorites found there (e.g., Schmitz 2013).

The Hällekis quarry

The Hällekis quarry is situated on the northwestern slope of Kinnekulle (Fig. 2). Today abandoned, the large limestone quarry supplied raw materials for the cement industry between 1892 and 1979. The quarry grounds are kept open as a recreational area. The outcrop encompasses the entire 'orthoceratite limestone' succession of Kinnekulle, and the exposed strata form one of the thickest and most complete sections through the Volkhov–Kunda interval in Baltoscandia. Successively younger strata, ultimately reaching into the basal Ryd limestone, are exposed towards the south (e.g., Lindskog 2014). The total thickness of the succession at the Hällekis quarry is c. 40 m.

For practicality, the quarry is here subdivided into five parts named Hällekis A through E (Figs. 4, 5). Hällekis A is the largest section, consisting of the main quarry area towards the south, in total comprising c. 1.5 km of laterally continuous rock exposure (Fig. 5A, B). A small gravel road runs along the rock wall to the east of the quarry lake in the southernmost part of the section, allowing for easy access to nearly the entire Lanna limestone–Holen limestone interval. The upper level in the southernmost part of Hällekis A hosts the youngest strata in the stratigraphic succession at the Hällekis quarry, including the entire Gullhögen Formation and the exposed Ryd limestone beds. A minor fault/fold structure is developed in the northernmost part of Hällekis A (Fig. 5C). The division between Hällekis A and B is drawn at a down step in the quarry floor just north of this structure. The

c. 15-m-thick succession of Hällekis B, which spans the lower Lanna limestone through the lower Holen limestone (including the 'Täljsten'), is similar to that of northernmost Hällekis A (Fig. 5D). Hällekis B is delimited northwards by a drape of loose debris. Hällekis C exhibits a c. 10-m-thick succession through the Lanna limestone (Fig. 5E). Hällekis D is a small, c. 2-m-thick, outcrop in the northernmost part of the quarry (Fig. 5F). There, in a ditch on the eastern side of the road leading into the quarry, the contact between the Tøyen Shale and the Lanna limestone is accessible near ground level. This part of the local stratigraphy is overall poorly exposed, and Hällekis D thus forms a small but crucial outcrop. Hällekis E forms a composite section along the western side of the quarry (Fig. 5G). This part mainly comprises a thin interval of the lower Lanna limestone, but an important subsection is found in a notch in the outcrop (E_1 in Fig. 4) where the contact between the Tøyen Shale and Lanna limestone is well exposed during times with low water level. Another subsection with very flatly cut walls (E_2) allows for detailed studies of the lower Lanna limestone.

Materials and methods

This study relies on several field campaigns undertaken during the last five years, wherein the 'orthoceratite limestone' was investigated throughout its distribution at Kinnekulle (Fig. 2). Numerous localities with coeval strata in other parts of Baltoscandia were also visited for comparative observations. Given its accessibility and illustrative stratigraphic succession, the Hällekis quarry was chosen as the main study locality at Kinnekulle. As such, it forms the 'type section' to which other localities are compared.

Several hundreds of samples, spanning the uppermost Tøyen Shale to lowermost Gullhögen Formation, were collected at Hällekis. A distinct hematite-stained discontinuity surface in the basal 'Täljsten', which is traceable across Kinnekulle, was used as a reference (0 m) level (see Lindskog et al. 2014). Measurements above this have been assigned positive numbers, and below negative numbers. A total of 220 thin sections were produced (excluding replicates) from the entire study succession. On average, this roughly corresponds to one thin section per 10–15 cm, or every second to third bed. Except where rock characteristics did not allow for it, samples were cut perpendicular to bedding in order to allow the study of grain orientation and packing, grading and other sedimentologic properties.

The thin sections were studied qualitatively and quantitatively in order to assess the overall depositional environment and variability of the succession at Kinnekulle. The relative amount of grains in relation to matrix and cement – i.e., carbonate texture – was determined through point counting via the grain-bulk method (see Dunham 1962; Jaanusson 1972). A total of 600 points were counted per thin section, using a grid covering the entire sample area. For assessing small-scale textural variability, every thin section was counted in sets of two 300-point sessions (each covering half of the sample area). Although they can be influenced by the same processes, distinction should be made between carbonate texture and grain size. Hence, the terms grain/particle size as used by Jaanusson (e.g., 1952, 1972) and others for the abundance of grains relative to matrix and cement (i.e. carbonate texture) is avoided. Grain size in carbonates is strongly affected by the taxonomic composition of rock-forming organisms and must be carefully assessed in relation to hydrodynamic and biodynamic processes in order to be meaningful (e.g., Olgun 1987). Grain size is not systematically measured here, although it is commented upon where deemed important.

The thin sections were further analyzed in terms of fossil grain assemblages. A modified form of ribbon counting (see Flügel 2010) was employed, wherein biogenic grains in continuous swaths (i.e. ribbons) aligned perpendicular to bedding were identified. All grains falling within the area of analysis were counted, each grain being counted only once. Seven categories were distinguished: Brachiopoda, Echinodermata, Gastropoda, Mollusca (other than identifiable gastropods), Ostracoda, Trilobita and Other. Notable reference literature includes Adams et al. (1984), Ulmer and Ulmer-Scholle (2006) and Flügel (2010). Also these analyses were subdivided into two sessions, i.e. in total 600 points per thin section, and individual counting sessions were halted when 300 individual grains had been identified. Thus, when including unidentified grains, analyses spanned more data points. Unidentified grains typically account for c. 10–15% of the observed grains and most represent small fragments referred to as Arthropoda indet. As the unidentified grains have negligible influence on the trends observed, for

clarity they were not included in the visual data presentations. In total, more than 280,000 points were registered during the quantitative analyses.

Results

Below follow descriptions of the main results of the field and thin-section studies, which are summarized in Figs. 6 and 7. Many of the lithologic and sedimentologic variations within the 'orthoceratite limestone' strata are clearly traceable between outcrops at Kinnekulle. Thus, except where specifically noted, described features are taken to occur throughout the table mountain.

General observations

Macroscopically, the 'orthoceratite limestone' is characterized by laterally extensive flat-lying beds separated either by marl interbeds or millimeter-thick shale seams (Fig. 8). Individual limestone beds vary in thickness between a few centimeters and a few decimeters. Some intervals are dominated by nodular limestone with poorly developed bedding. Brown and red hues dominate the rock color, with gray, yellow and green being subordinate. Fossils typically are rare, and most specimens are fragmented and/or poorly preserved. Articulated specimens occur among multipartite fossils, but they nonetheless tend to be difficult to extract. Trilobites and cephalopods variably dominate the macrofauna. Many beds are visibly bioturbated internally, but extensively bioeroded bedding surfaces are relatively rare. The most common ichnofossils include *Balanoglossites*- and *Planolites*-like burrows/borings (see Knaust & Bromley 2012; Knaust & Dronov 2013).

Microscopically, the 'orthoceratite limestone' is characterized by a microcrystalline matrix strewn with variable amounts of skeletal grains (Figs. 9, 10). The original matrix consists of calcareous mud mixed with fine-grained siliciclastics. Patches of recrystallized matrix are common, especially in connection with bioturbation and hardground surfaces. Voids and shelter pores filled with cement are common, and deposits that resemble vadose silt (see Flügel 2010) occur (Fig. 9L). Porosity is consistently negligible. Grain surfaces typically appear abraded and/or corroded. Sand-sized siliciclastic grains are rare, and mainly comprise rounded quartz and mica flakes. Coarser non-carbonate matter is very rare. Some beds are rich in authigenic minerals, typically limonite, glauconite and pyrite (Figs. 9B, K, 10B, D, J, L). Bioturbation has commonly entrained grains in 'stringers' that form whirling patterns throughout the rock. This has effectively homogenized grain distributions within most beds, but both normal and reverse grading occurs. A typical limestone in the studied succession can be described as a well-bioturbated skeletal wackestone (see Dunham 1962). Packstone occurs patchily throughout and dominates in some intervals. Only rarely does the grain abundance fall below the 10% limit that marks true mudstone texture, and significant amounts of grainstone only occur in a few thin intervals. Marly and nodular strata tend to have finer carbonate texture than the denser limestone beds, but exceptions occur. Fossil grain assemblages mainly consist of trilobite, ostracod and echinoderm debris, although gastropods and brachiopods occasionally are abundant (see Eriksson et al. 2012; Lindskog et al. 2015). Minor fossil constituents include sponge spicules, acritarchs, chitinozoa, scolecodonts, agglutinated foraminifera and indeterminate organic fragments. Sponge spicules are likely underrepresented in the data (Figs. 6, 7), as this grain type is often difficult to identify in the microcrystalline matrix unless favorably oriented. Cephalopod debris dominates among mollusk grains other than gastropods, with hyoliths and bivalves occurring only rarely.

Throughout much of the succession, there is a meter-scale cyclic/repetitive pattern of relative coarsening and fining of carbonate textures that coincides broadly with changes in fossil grain assemblages, which fluctuate between distinctly arthropod-dominated and more varied ('diverse') faunas dominated by echinoderms and mollusks (Figs. 6, 7). The biotic variations are more visually pronounced in thin sections than is suggested by Figs. 6 and 7, as echinoderms tend to produce relatively large grains (see Jaanusson 1972). Microfacies show only limited lateral variation within individual beds, as is illustrated by the continuity of trends between the Hällekis subsections (Fig. 6).

Diagenetic features are occasionally common, especially in marly and nodular strata. Sinuous solution seams filled with insoluble siliciclastic matter occur abundantly in these beds (Figs. 9D, F, N, 10C). Stylolites also occur, especially in the middle part of the succession. There has certainly been some loss of carbonate material during diagenesis; solution has evidently destroyed skeletal grains and primary sedimentary structures, and truncation of fossils sometimes indicates removal of strata at the

centimeter scale. Fitted fabrics commonly occur along solution seams. Although solution seams often coincide closely with partings between beds at the macroscopic scale, these horizons do not necessarily reflect primary bedding surfaces. Where partings do coincide with primary bedding, surfaces have rarely escaped significant diagenetic alteration and few primary characteristics can be identified. Even among evidently synsedimentarily lithified horizons, many lack signs of having been directly exposed at the seafloor.

Sedimentary and biotic variations

Tøyen Shale

The uppermost Tøyen Shale is characterized by greenish gray mudstone and shale, in places with a rusty appearance. At the Hällekis quarry, the uppermost part of the formation hosts a number of c. 2–5-cm-thick and discontinuous grayish limestone beds (Figs. 6, 8A, B. These all show a mudstone texture, wherein pervasive diagenetic recrystallization of the matrix hampers identification of small skeletal grains (Fig. 9I). Rounded glauconite grains occur sparingly throughout, with concentrations tending to increase toward the top of individual beds. The uppermost limestone bed is characterized by a mottled color, varying between gray, brown, red, yellow and green, and numerous rounded intraclasts occur at its base. The limestones in the Tøyen Shale are nearly barren of skeletal grains, and fossil 'grains' are dominated by acritarchs (Fig. 6). Identifiable skeletal grains mainly include fragmented arthropod sclerites and phosphatic brachiopods. The proportion of skeletal grains increases toward the top of the formation, but remain rare. The macrobiota is poor, and only a few small indeterminate brachiopods and fragments of organic material (graptolites?) were found. However, ample biologic activity is recorded via ichnofossils; numerous (sub-)vertical tube-shaped burrows and/or borings occur, and increase in number upward in stratigraphy (Fig. 9A). Glauconite grains and coarse barite crystals are common burrow fills.

The boundary between the Tøyen Shale and the Lanna limestone is here placed at the level where the shale facies disappears completely and dense reddish limestone commences (Fig. 8A, B). The boundary interval varies slightly across Kinnekulle, as the proportion of limestone interbeds in the uppermost Tøyen Shale increases towards the southeast. This results in a more gradual lithologic transition between the formations, but a distinct difference in weathering resistance allows for accurate identification of the formational boundary (see Fig. 8B).

Lanna limestone

The lowermost Lanna limestone is characterized by dense limestone of mudstone to wackestone texture (Figs. 6, 8A, B). These beds are reddish brown in color at the Hällekis quarry, but they are more grayish at some other localities of Kinnekulle. The basal beds host a succession of limonite-stained hardground surfaces replete with (sub-)vertical pits that probably represent secondarily corroded/eroded borings (Figs. 8C, 9B, J). Millimeter-sized carbonate intraclasts occur at the base of the lowermost Lanna limestone bed. Variably rounded, sand-sized glauconite grains are abundant, especially in borings/burrows (Fig. 9K), but concentrations decrease in overlying beds and glauconite becomes insignificant (stray grains persist). The limonitic stain of hardgrounds decreases upward through the strata, and well-developed hardgrounds become uncommon c. 0.5 m into the Lanna limestone. This change is associated with a shift in the ichnofauna, from a predominance of hardground borings (*Gastrochaenolites*-like domichnia) via firmground (*Balanoglossites*-like domichnia/fodinichnia) and into softground burrows (*Planolites*-like fodinichnia; see Knaust & Bromley 2012). There is a gradual shift towards coarser carbonate textures upward (Fig. 6). Fossil grain assemblages in the lower Lanna limestone are distinctly dominated by arthropods, mainly trilobite sclerites, but especially echinoderm grains become more common upward. In places, the lowermost Lanna beds are buckled into dome-like structures (Fig. 8B). Geopetal indicators show that the buckled surfaces were initially horizontal (Fig. 9B). Overlying beds are undisturbed and horizontally stratified, and contact the 'domes' at oblique angles. Dome-like structures occur in rock walls cut in various cardinal directions, and occasionally also higher up in the succession.

A remarkably flat discontinuity surface occurs c. 2.3 m above the base of the Lanna limestone and it is traceable throughout the Hällekis quarry (Figs. 6, 8D). Several surfaces above this level are also unusually flat, but increasingly less so. *Balanoglossites*-like burrows/borings with limonitic lining are

common in these beds, and are most concentrated below the top surfaces. These ichnofossils were clearly produced in a partially to fully lithified substrate and were later filled with sediment from above, or with calcite cement (Fig. 9L). At the Hällekis quarry, there is an interval of unusually marly and finely nodular limestone c. 4 m into the Lanna limestone that facilitates correlation along the kilometer-long outcrop (Figs. 6, 8E). Precise correlation over longer distances is not entirely straightforward, however, as the marly band temporarily thins out north of Hällekis A and reappears further north. Nevertheless, its overall sedimentologic characteristics are persistent and this level is associated with an increase of sessile benthos in the fossil grain assemblages.

The main part of the Lanna limestone is quite easily recognized in the field by its characteristic bedding, which shows alternation between relatively thin, firm limestone beds and marly, easily eroded interbeds (Fig. 8F). This alternation takes place with some regularity, each limestone-marl couplet being approximately a decimeter thick; the marly portions are generally thinner than the limestone that they grade into upward. This part of the formation is characterized by gradual alternation between mudstone and wackestone at the meter-scale, with some coarser-textured beds interspersed (Fig. 6). The initiation of the limestone-marl alternation is associated with an increase of mollusks (mainly gastropods) and echinoderms within grain assemblages. The upper part of the limestone-marl interval contains fossil-rich beds with many articulated (enrolled and prostrate) trilobites.

The upper Lanna limestone records a successive coarsening of carbonate textures (Fig. 6). At the macroscopic scale the limestone beds start to form thicker banks and rugged hardgrounds with limonite-stained top surfaces become common (Fig. 9G, H). Abundant *Balanoglossites*-like burrows occur beneath these surfaces, and several beds are red-yellow-gray-mottled in color. Hematite staining is conspicuous in the uppermost beds. Limonitic hardgrounds are most common close to the Lanna limestone–Holen limestone boundary. Several of the transitional beds are strewn with ferruginous coated grains and stromatolite-like formations occur (Fig. 9P). Some of these beds show dissolution effects, but there is no clear evidence of subaerial exposure. Variably rounded intraclasts and clearly reworked fossils are common in the uppermost Lanna limestone and the basal Holen limestone (Fig. 9G, H).

Holen limestone

The transition between the Lanna limestone and the Holen limestone is marked by a change from dense into marly nodular limestone. The basal Holen limestone is thus distinguished in the field as a relatively easily weathered interval (Fig. 8G; see Lindskog et al. 2014). This lithologic shift is associated with a marked fining of carbonate textures and a return to arthropod-dominated grain assemblages (Fig. 7). The marly limestone is poorly bedded, but more competent beds occur regularly. These beds host numerous limonite-lined *Balanoglossites*-like burrows/borings, many of which have been filled with coarse calcite. Wavy hematitic seams, some widely traceable, occur in some beds. Carbonate textures coarsen significantly upward through the strata. Fossil grain assemblages progressively become more varied, with the reintroduction of numerous echinoderm grains associated with gastropods and brachiopods. Gastropods and other mollusks reach a maximum in abundance just below the gray-colored 'Täljsten' and remain abundant well into the Holen limestone. Dense accumulations of cephalopod conchs occur in several horizons (see Lindskog et al. 2015). The 'Täljsten' is underlain by c. 0.5 m of beds strongly enriched in hematite and unusually deep rusty red in color (Fig. 8K).

The 1.5-m-thick gray 'Täljsten' clearly deviates from the typical appearance of the local 'orthoceratite limestone' (Fig. 8G, H, J). The lower 'Täljsten' is rich in glauconite, occurring as discrete grains with signs of reworking and as shell fillings evidently formed *in situ* (Fig. 10B, C, J). Numerous macroscopic crinoid holdfasts occur on some bedding surfaces in the basal 'Täljsten' (Fig. 8I), but corresponding macroscopic echinoderm debris is enigmatically missing. The middle part of the 'Täljsten' contains centimeter-thick seams of dark gray clay/silt intercalating with slightly nodular limestone. Pyrite dust is occasionally common (Fig. 10J). Numerous phosphate-enriched firmground and hardground surfaces occur throughout the 'Täljsten' (Fig. 10I). A millimeter-thin phosphatic 'crust' has commonly been penetrated by burrowing organisms, which apparently reached into a softer substrate below. Beds packed with *Sphaeronites* cystoids occur in the middle and upper part of the 'Täljsten', and articulation of these fossils forms unambiguous evidence of rapid induration of their

host sediment. Many incompletely sediment-filled specimens are eroded and/or crushed in their upper part. Stray cystoids, many of which are clearly reworked, occur at least a meter above the 'Täljsten'. The uppermost 'Täljsten' is characterized by abundant limonitic grains, in the transitional interval between gray and red limestone (Fig. 10D, L). Much of the limonite appears to represent oxidized glauconitic compounds, with grains exhibiting variable degrees of limonitization that acted from the outside and inwards. Although red limestone recommences, several sedimentologic details remain similar to those of the 'Täljsten'. Overall, the 'Täljsten' and the overlying c. 3.5 m of strata stand out as exceptionally coarse-textured (Fig. 7). These beds host the most diverse fossil grain assemblages and also form the most fossil-rich interval macroscopically. This coincides with several signs of a more biologically and hydrodynamically active environment at the seafloor. Many hardgrounds are visibly eroded and intraclasts, often centimeter-sized, are common (Fig. 10D). Several beds host thin coquinoid horizons, with coarse shell debris of variable orientation (concave/convex up) and patches of grainstone (Fig. 10E). Cephalopod conchs show preferential alignment towards the south and siphuncular orientations vary (Fig. 8K). Centimeter-sized oncoids occur sporadically throughout the Holen limestone, but they are most abundant in the lowermost 'Täljsten'. Variably sized coated grains (ferruginous 'ooids' and/or micro-oncoids) are concentrated at several levels (Fig. 7; see Lindskog 2014). Thin stromatolite-like structures are found on some bedding surfaces (Figs. 8K, L, 10M) and numerous microborings in skeletal grains indicate an unusually active endolithic microbiota (Fig. 10H, N). Coarse barite is common in the 'Täljsten' and overlying beds, and many macrofossils are filled with crude oil.

The upper Holen limestone is characterized by a gradual return of marly interbeds and the uppermost part even shows alternation between thin, sometimes discontinuous and nodular, limestone beds and calcareous shale (Figs. 7, 8M). This change is associated with a fining of carbonate textures and an apparent decrease in macrofossil abundance. *Planolites* burrows, preserved essentially undistorted in three dimensions, occur alongside *Thalassinoides*. Many beds show typical storm bed characteristics, with normal grading and distinct bimodality in grain size. Locally, dense accumulations of large cephalopod conchs and trilobite sclerites occur (Fig. 8O). Several limestone beds in the uppermost c. 3.5 m are densely populated by circular burrows/borings, typically c. 1 cm in diameter and 1–2 cm deep (Fig. 8N), many of which contain coarse barite crystals. Although variable in details, these pits probably all represent the same ichnogenus (*Conichnus* or shallow *Gastrochaenolites*?). Many shelly fossils are enveloped in a ferruginous crust and concretions are common (Fig. 8O). Grain assemblages in the uppermost Holen limestone are impoverished and strongly dominated by trilobite fragments (see Fig. 7). Stromatolite-like lamination occurs in the uppermost bed (see Lindskog 2014). The top of the Holen limestone is indicated by an exceptionally flat discontinuity surface and a change from rusty red into dominantly gray rock color (Figs. 8P, 10G; see Holmer 1983). Depressions and sediment-filled cavities (secondarily corroded/eroded burrows?) in the discontinuity surface contain numerous ferruginous ooids and occasionally rounded quartz grains. The surface itself is intermittently draped with a thin laminated phosphatic crust and similar crusts occur with variable orientation in the walls and roofs of cavities (Fig. 10O). The beds bracketing the Holen–Skövde boundary contain numerous millimeter-thick vertical cracks filled with calcite and rimmed by hematitic staining that were evidently formed after complete lithification.

Skövde limestone–Gullhögen Formation

The Skövde limestone is represented by a mere decimeter-thick grayish wackestone (Figs. 8P, 10G). A thin lag, essentially a packstone, consisting mainly of ferruginous and phosphatic ooids is found at its base (see Sturesson 1989). In places, the limestone matrix has been recrystallized into a meshwork of variably oriented calcite aggregates (similar to 'ant-egg spar' *sensu* Lindström 1979). The succeeding Gullhögen Formation comprises thin, commonly discontinuous, beds of gray to light brown impure limestone alternating with calcareous shale (Fig. 8P; see Jaanusson 1964). The lowermost part of the formation consists of a few relatively dense beds of wackestone, sometimes with notable amounts of ferruginous grains and ooids. Mudstone intercalated with calcareous shale occurs above. The fossil grain assemblages of the Skövde limestone and basal Gullhögen Formation are dominated by trilobite debris, but there is an increase in organic-walled fossils (acritarchs and graptolites) upward.

Discussion

Features and formation of the 'orthoceratite limestone'

Although the 'orthoceratite limestone' appears to be quite homogeneous at the macroscopic scale, closer inspection reveals many details that distinguish different parts of the succession at Kinnekulle. Several such features occur across the table mountain and some can even be traced to other parts of Sweden and neighboring countries.

The local depositional environment wherein the 'orthoceratite limestone' formed at Kinnekulle clearly varied through time, but lateral variations were consistently limited. Thorough bioturbation and diagenetic processes have typically obscured or obliterated primary sedimentary structures, leading to some difficulty in assessing the overall depositional environment. Moreover, early lithification in carbonate environments (and also microbial mats) quickly stabilizes the seafloor and hinders formation of sedimentary structures that may reveal details about the hydrodynamic conditions and processes. For most of the interval studied here, however, the environment at the seafloor appears to have seen little disturbance from wave action and coarser beds likely reflect storm events (see also Hadding 1958). There is a common contrast between a very fine-grained matrix, and coarse skeletal fragments and intraclasts. Intervals dominated by packstone, and the occasional grainstone horizons, record higher-energy conditions at the seafloor and in many cases –especially in the coarse-textured interval that embraces the 'Täljsten' – wave action seems to have played an important role during the formation of the strata. This is indicated by a smaller proportion of matrix in the rock, more consistent rounding of grains, abundant intraclasts, erratically oriented siphuncles in cephalopods, and occasionally also the presence of oncoids (see Lindskog 2014). In terms of absolute numbers, the water depth in the Kinnekulle area probably varied between near zero and some tens of meters during the time interval represented by the studied succession.

The limonitic hardgrounds in the lowermost Lanna limestone were described in detail by Lindström (1979). This interval coincides closely in character and time with a regionally developed hardground complex colloquially referred to as 'Blommiga Bladet' ('the Flowery Leaf/Sheet') and may be considered as an equivalent. However, biostratigraphic details reveal that the hardgrounds at Kinnekulle do not coincide precisely with the Billingen–Volkhov boundary, as is otherwise typical for 'Blommiga Bladet' (Bergström & Löfgren 2009). This apparent diachroneity is also seen in the Billingen-Falbygden area, c. 50 km southeast of Kinnekulle (Olgun 1987) and is likely an artifact of differential deposition and erosion across the paleobasin. Events related to the formation of 'Blommiga Bladet' are possibly reflected already by the multi-colored limestone bed in the uppermost Tøyen Shale at Kinnekulle. Hardground formation in the 'orthoceratite limestone' at Kinnekulle appears to have been most pronounced in the earliest stages of sea level rise (see below). This transitional interval entailed severe sediment starvation due to winnowing and bypassing of sediment.

Sedimentary structures identical or closely similar to the 'domes' in the lower Lanna limestone at Kinnekulle have been documented from other parts of Sweden and with different interpretations. Lindström (1963) interpreted them as folds formed as a result of gliding of the seafloor, whereas van Wamel (1970; cf. Lindström 1971b) considered them as dome-shaped structures formed via migration and local accumulation of underlying sediment. Stephansson (1971) suggested them to be the result of diapir-like processes. Essentially, however, all authors agreed that the structures were synsedimentarily formed due to deformation of the seafloor and this study support this. Regardless of detailed genetic interpretation, their overall properties indicate a dome-like rather than fold-like shape (see above). The structures share many similarities with so-called Hecker-type mud mounds, which occur in coeval strata in the Baltic Region and are interpreted as biologically formed (Fedorov 2003).

The thin-bedded limestone-marl alternation characterizing much of the Lanna limestone at Kinnekulle (Fig. 8F) is clearly distinguishable also in other parts of Sweden, most notably in the Billingen-Falbygden area and the type area of the topoformation in the province of Närke. The geographically widespread development of this bedding indicates some primary rhythmicity in sedimentation patterns (see De Geer, 1941), the record of which has been enhanced during diagenesis (e.g., via selective compaction; e.g., Bathurst 1987). Curiously, the color and thickness of the Lanna limestone varies drastically between Kinnekulle and the nearby Billingen-Falbygden area, where the Lanna limestone is mainly light gray in color and hence traditionally referred to as the 'Vitsten' ('White stone'; Westergård 1928).

The 'Täljsten' forms a regionally traceable 'event' level and thus an important reference level in Baltoscandian stratigraphy, although superficial characteristics across this interval may vary between localities (e.g., Eriksson et al. 2012). Some areas of Sweden show remarkable similarities to the succession at Kinnekulle and the 'Täljsten' is thus immediately recognizable in the Billingen-Falbygden area, where it is traditionally referred to as the 'Blåsten' ('Bluestone'; Westergård 1928), and southern Öland in the Baltic Sea. These areas show a closely similar facies development through the 'Täljsten' interval and the beds directly below are visibly stained by hematite, as at Kinnekulle (see also Tjernvik & Johansson 1980; Rasmussen et al. 2013). Many localities are furthermore associated with *Sphaeronites* beds (see Regnéll 1945, 1948; Paul & Bockelie 1983). Such beds also occur in coeval strata in other parts of Sweden and this regional cystoid acme probably reflects opportunistic colonization. The gray, glauconitic and limonitic limestone facies of the 'Täljsten' shares many similarities with those more typical for the Baltic area. This facies, which is associated with relatively high fossil diversity, appears to have developed in a time-transgressive manner throughout Sweden. For example, it occurs already in the upper Volkhovian in northern Öland (Bohlin 1949), and a similar facies occurs in coeval strata in Närke (Löfgren 1995). It then entered the succession in the provinces of Jämtland (Karis 1998) and Dalarna (Hessland 1949; Jaanusson 1982c) close to the Volkhov–Kunda boundary. The 'Täljsten' marks the culmination of this facies migration after which red strata became more widespread throughout Baltoscandia, essentially in reverse order geographically compared to the introduction of the gray beds. From a regional perspective, the gray facies apparently wandered from shallower into deeper – or, rather, proximal into distal – settings through time. Indeed, several proxies indicate that the 'Täljsten' is the manifestation of a drastic lowering of the sea level and thus reflecting more proximal facies than the typical reddish limestone at Kinnekulle (e.g., Tinn & Meidla 2001; Mellgren & Eriksson 2010; Eriksson et al. 2012; Lindskog 2014; Lindskog et al. 2015). Proximity and distance to paleoshorelines must not necessarily correspond directly to absolute water depths, but regional-scale sedimentary dynamics (i.e. patterns of deposition) indicate a strong influence from sea level on sedimentary characteristics (e.g., Männil 1966; Jaanusson 1973; Põlma 1982). However, dominantly gray carbonate rocks are found on both sides of the Kinnekulle area in a proximal–distal transect (~east–west in present-day directions; e.g., Hadding 1958). On the proximal side, gray coloring was largely facilitated by early lithification and subsequent preservation of organic matter and reduced compounds such as glauconite and pyrite. The possibility to attain overall reducing conditions was probably enhanced by a relatively high productivity and subsequent flux of organic matter in shallower waters. On the distal side, gray grading into blackish coloring typically resulted from decreased oxygenation and stagnant conditions at the seafloor, with subsequent preservation of organic matter and reduced compounds (mainly pyrite). Red-colored strata clearly span a range of depositional depths, possibly from intertidal to deep subtidal (Figs. 6, 7, 9, 10; see Reyment 1970; Jaanusson 1973; Larsson 1973; Põlma 1982; Karis 1998; Lindskog 2014). Distally, the basin normally hosted siliciclastic mudstone and shale. An increase in terrigenous matter is seen also towards the proximal part, where the carbonate deposits tend to be marly, but the main weathering source(s) may differ (e.g., Jaanusson 1973). This overlap in appearance and composition of the regional rocks highlights the need for caution when deducing relative depth of deposition from superficial characteristics (cf. Nielsen 2004; Dronov et al. 2011).

Despite the aforementioned developmental similarities of the 'orthoceratite limestone' at the regional scale, there are distinct differences in its properties between different parts of Sweden and different stratigraphic levels at the local scale. Hence, the 'orthoceratite limestone' should not be regarded as a single, homogeneous facies but rather a (mega-)suite of superficially similar cool-water carbonate facies that can even be distinguished into several subfacies both laterally and temporally. Only in the broadest sense does the 'orthoceratite limestone' represent a homogeneous ('stable') environment at the ancient seafloor, and its differing characteristics – however subtly expressed – signal important variations in the depositional environment. The overall fine-grained nature of the limestone, with its typically large proportion of carbonate mud, intuitively suggests a relatively low-energy (and deep-water) hydrodynamic regime in the Ordovician Baltoscandian paleobasin. However, deposition of carbonate mud can take place in rather variable hydrodynamic conditions (see Schieber et al. 2013) and the spatiotemporal variability of microfacies and fossil content within the 'orthoceratite limestone' indeed indicates that it was deposited across a range of paleoenvironments while still maintaining its overall macroscopic characteristics. The most important factor for the long-

term establishment and regional dominance of the 'orthoceratite limestone' facies appears to have been the severe lack of terrigenous sediment input to the paleobasin rather than any specific physical parameters (e.g., depth, currents, temperature). The low production potential of the oligotrophic cool-water (temperate) carbonate system actually necessitated a restricted influx of siliciclastics for carbonate deposition to prevail. Consequently, carbonate production was in constant competition with siliciclastics (Jaanusson 1973; cf. Nielsen 1995) and any change in the balance between the two could result in drastic changes in facies distribution. Much of the regional facies zonation may reflect distance from weathering sources rather than water depth.

Microfacies as a paleoenvironmental proxy

The Kinnekulle area appears to represent a relatively deep-water setting within the Baltoscandian paleobasin, but it evidently was shallow enough to react to environmental fluctuations. This is manifested by the microfacies variability, wherein both carbonate textures and fossil grain assemblages vary in an apparently cyclic manner (Figs. 6, 7). There is also a long-term pattern of change in carbonate textures throughout the succession, from finer into coarser textures and back again. The typically smooth patterns in the microfacies data (i.e., lack of abrupt shifts) indicate an overall slow but stable sedimentation over longer time scales, but individual beds may have been deposited rapidly. While the condensed nature of the 'orthoceratite limestone' limits temporal resolution it provides robustness to paleoenvironmental interpretations as the associated time averaging results in homogenized bed content and few 'erratic' extremes (e.g., seasonal/annual/decadal 'snapshots') in the data. A consistent mixture of soft-bottom and hard-bottom faunal components (see Nordlund 1989) records the change from loose to firm sediment of individual beds. Thus, provided large enough sample area coverage and number of counts, quantitative microfacies analysis accurately captures the average composition of any given bed. The condensation comes at a cost, however, as it necessitates high sampling resolution in order to document the paleoenvironmental development in any detail.

A comparison between the microfacies data from Kinnekulle and regional depositional patterns (e.g., Männil 1966; Jaanusson 1973; Põlma 1982) indicates a strong connection between carbonate textures and sea level. Intervals with wide areal distribution of strata throughout Baltoscandia (i.e. indicative of high sea level) are associated with finer carbonate textures at Kinnekulle, whereas intervals characterized by widespread unconformities and limited deposition (i.e. low sea level) are associated with coarser textures. Hence, the cool-water 'orthoceratite limestone' appears to have behaved much like 'model' siliciclastic sedimentary systems (e.g., Schlager 2005), in that carbonate texture varied with depositional depth as particle size of siliclastics does. The validity of this general principle is reinforced by a general coarsening of carbonate textures towards arguably shallower-water depositional environments within coeval strata and vice versa for deeper-water environments (e.g., Jaanusson 1973; Põlma 1982; Olgun 1987; Nordlund 1989). This is likely a combined effect of changes in bioproductivity and hydrodynamic activity. The 'orthoceratite limestone' differs significantly from siliciclastics in the behavior of the large-scale sedimentary system, however, as most sediment production (in terms of volume) appears to have taken place during relatively high sea level. This is a common feature of carbonate ramp, or ramp-like, systems, as higher sea level maximizes the area available for biologic production and carbonate accumulation but minimizes terrigenous input (e.g., Schlager 2005). Still, as cool-water limestones largely comprise biologically and mechanically eroded skeletal material, carbonate deposition may partly have been positively influenced by lower sea level. This can result in differential sedimentation along depth transects. It must be stressed that the constituents of carbonates are mainly autochthonous or parautochthonous in origin, as opposed to siliciclastics, which consist of materials transported into their final resting place.

Fossil grain assemblages also appear to be influenced by water depth (likely indirectly so). In particular, trilobites show an inverse relationship to echinoderms in relative abundance and these groups may be considered as end members in a spectrum of biotic variability; trilobites dominate in the arthropod-dominated grain assemblages and echinoderms in those more varied. From a regional perspective, trilobites appear to represent more distal biofacies than echinoderms do (e.g., Olgun 1987; Rasmussen & Stouge 1995) and variations in grain assemblages thus reflect migration of facies belts along bathymetric gradients. Consistent regional faunal patterns and the rarity of long-distance transport of skeletal material (e.g., Brett & Baird 1986) indicate paleoecologic zonation across the

paleobasin. Consequently, the echinoderm-rich assemblages are likely to represent relatively shallow and the trilobite-dominated assemblages deep water (but see below). An inverse situation is also possible, should shallower conditions be related to a brackish and/or stagnant environment and deeper conditions related to more normal salinity and better circulation. Such a case appears unlikely here, however, given the consistent presence of echinoderms regionally. The modal composition of a fossil grain assemblage is not necessarily reflective of the paleoecosystem, at least not in terms of number of individuals of different organisms (furthermore, soft-bodied organisms are typically missing; but see Eriksson et al. 2016). Still, fluctuations in the relative abundance of fossil grains in thin sections from Kinnekulle appear to reflect changes in the macroscopic biota quite well (see Eriksson et al. 2012; Lindskog et al. 2015; cf. Jaanusson 1972). Microbiofacies thus record larger-scale changes, but the relative abundance of different fossils is often significantly offset compared to macroscopic counterparts.

The variations seen in the microfacies data from Kinnekulle are clearly traceable to other parts of Sweden (see Lindström & Vortisch 1983; Olgun 1987; Nordlund 1989; Lindskog et al. 2015) and likely other parts of Baltoscandia (Põlma 1982), although detailed comparisons are hampered by differing analytic approaches and biostratigraphic uncertainties.

Given the above, microfacies form a proxy for relative sea level (or, local water depth) and can thus be utilized for the construction of sea level curves. However, the perceived changes in sea level sometimes differ between carbonate textures and fossil grain assemblages. This likely reflects influence from substrate conditions upon benthic communities and long-term changes in overall ecosystem composition, and care should be taken when comparing intervals with different (sub-)facies and of vastly different age. Essentially, carbonate texture appears to be a better indicator of absolute water depth than fossil grain composition is, but the latter better records higher-frequency changes in the depositional environment.

Sea-level changes

Using the interpretative principles described above, a sea level curve was produced for the studied interval (Fig. 11). Overall, the resulting sea level curve is in excellent agreement with that recently presented by Rasmussen et al. (2016) and also agrees well with other high-resolution curves. Still, some parts of the stratigraphic succession remain less easily defined in terms of relative depth and such intervals are treated in more detail below. Differences between previous studies (e.g., Dronov et al. 2011; Nielsen 2011) in the detailed interpretation of the sea level for some parts of the concerned interval likely stem from differential sedimentation across the paleobasin, wherein different parts saw maximum carbonate deposition at different times (see above). Comparisons at the global scale are hampered by insufficient resolution, but a correspondence of overall trends indicates a strong eustatic signal within the data.

After a notable drop at the Billingen–Volkhov/Floian–Dapingian transition, which essentially halted deposition across the Baltoscandian paleobasin and resulted in the formation of 'Blommiga Bladet' and equivalent horizons (see Bergström & Löfgren 2009), the sea level appears to have become quite high in the earliest Volkhovian. Superimposed upon higher-frequency variations, including some notable drowning events that seem to be regionally traceable, the sea level then gradually fell until a new lowstand was reached close to the Volkhov–Kunda boundary. This level is typically marked by a disconformity in proximal areas of the paleobasin (e.g., Hints et al. 2012; Meidla et al. 2014), but the transition between the stages is relatively complete at Kinnekulle. The earliest Kundan was characterized by relatively deep water, but this rapidly gave way to a renewed shallowing that culminated during the formation of the 'Täljsten' and its enclosing coarse-textured rocks. This interval marks the shallowest conditions in the studied succession, but the overall trend throughout it is one of rising sea level, as manifested through increasingly pronounced drowning episodes. Still, the sea level appears to have remained relatively low for a prolonged period of time (see also Nordlund 1989) and the microfacies data do not indicate any remarkable drowning in the *A. expansus–A. raniceps*/*L. variabilis*–Y. *crassus* boundary interval, as is often discussed in the literature (e.g., Nielsen 1995, 2004, 2011; Kröger & Rasmussen 2014). The first signs of truly significant drowning (at Kinnekulle) occur c. 1.5 m above the 'Täljsten', but longer-term establishment of deeper-water conditions did not occur until c. 3 m above it (Fig. 7). The latter level coincides closely with the last occurrence of *Anthoceras vaginatum*, a cephalopod species that is characteristic for relatively

shallow-water environments of the Baltoscandian paleobasin (Kröger & Rasmussen, 2014). The diachronous occurrence of *A. vaginatum* throughout Baltoscandia highlights a weak point in the traditional subdivision of the regional strata (the term Vaginatum Limestone in older literature is dubious) and for biostratigraphy in general. The species appears to have tracked environments with appropriate water depth and its last occurrence at Kinnekulle marks the reestablishment of deeper-water conditions (cf. Kröger & Rasmussen 2014). Conflicting data and interpretations concerning the middle Kundan may indicate that this was a time of large amplitude in sea level variations. The shallowing that characterizes the latest Volkhovian to middle Kundan was likely a global phenomenon (e.g., Lindström & Vortisch 1983; Chen & Lindström 1991; Nielsen 2004; Rasmussen et al. 2009; Wu et al. 2014).

Sea level rose quite steadily throughout later part of the Kundan and ultimately reached the highest conditions of the studied interval. The strata at Kinnekulle from this time indicate a distal environment with occasional influx of coarser material during storms, with an environment at the seafloor unable to sustain any substantial amount of organisms. Several aspects of the regional sedimentary development thereafter indicate a prolonged time with high sea level, although the record is somewhat ambiguous. The absence of Aserian deposits and the sparse Lasnamägian at Kinnekulle stands out as an anomaly from a regional perspective. The long hiatus at Kinnekulle is typically explained as a time of very shallow-water conditions, perhaps even with subaerial exposure (e.g., Jaanusson 1964; Holmer 1983; Lindskog 2014). However, provided isostatic/tectonic stability, this explanation is problematic, as the latest Kundan contrastingly was the first time that many parts of the Baltoscandian paleobasin hosted any (significant) deposition after variably long hiatuses. Most notably, after a more or less uninterrupted hiatus since the early or middle Cambrian, sedimentation recommenced during this time in the central parts of today's Baltic Sea (Thorslund & Westergård 1938; Thorslund 1958) and also in northwestern Estonia, which had seen very limited deposition since the Tremadocian (e.g., Meidla et al. 2014). Thereafter, while there was little or no deposition in the Västergötland area and along a belt going southwards via Bornholm (Jaanusson, 1972) and Poland (Dzik & Pisera 1994) into Ukraine (Saadre et al. 2004), surrounding areas – notably including those that were arguably shallower – hosted significant sediment deposition throughout the Aserian and Lasnamägian (e.g., Männil 1966; Jaanusson 1973; Wu et al. in press). This shift in the depositional patterns throughout Baltoscandia may reflect that such a high sea level was reached that complete sediment starvation ensued in areas with hiatuses, or that it brought these into parts of the shelf that were exposed to unusually energetic currents. An alternate explanation may be that epeirogenic movements or movements related to the incipient Caledonian orogeny led to differential flexing of the crust, which entailed shallowing in the areas with hiatuses and deepening in the surroundings. Whatever the case, tectonic influence on the regional sedimentary development (and sea level) cannot be excluded. Areas with deposition show signs of significant fluctuations in sea level that are not recorded in the Kinnekulle area due to the hiatus (e.g., Jaanusson 1973; Nielsen 2004). Coeval hiatuses in Baltoscandian, Chinese (see Schmitz et al. 2010; Zhang & Munnecke 2016) and South American (see Albanesi et al. 2013) sections, together with a coincidence with the Middle Ordovician Carbon Isotopic Excursion (MDICE; Ainsaar et al. 2004, 2010), merit detailed investigation of rocks from this time interval. Such studies must naturally be undertaken elsewhere than Kinnekulle.

Regional and global comparisons indicate shifts in sea level that exceed 100 m in amplitude in the studied interval and several proxies show some indication of cyclicity in their variations (e.g., Lindström & Vortisch 1983; Rasmussen et al. 2016). Cyclic variations are apparent at several frequencies and with variable amplitude within the microfacies of the 'orthoceratite limestone' at Kinnekulle. This, together with the commonly steady pacing and symmetric patterns in the data, indicate astronomically driven climate change – i.e. Milankovitch cyclicity – as the driver behind the sea-level changes. Confident testing of such a scenario is hampered by poor temporal constraints on the studied succession. This problem pertains both to the overall time scale throughout this interval and the understanding of the time distribution within it. Using current age estimates for the Volkhovian–Kundan time interval (Gradstein et al. 2012; Lindskog et al. 2017), counting of the main peaks in the microfacies data indicates cyclicity on the order of 250–400 ka. This implicates orbital eccentricity within the concept of Milankovitch cyclicity (e.g., Hilgen et al. 2015), but much better temporal control is needed to validate any claim of astronomic influence on the studied succession.

Conclusions

The 'orthoceratite limestone' is much more variable than is suggested by its overall homogeneous appearance. The macroscopic and microscopic characteristics of the succession at Kinnekulle reveal information about the paleoenvironmental development during the Middle Ordovician, and microfacies show apparently cyclic variations among both abiotic and biotic components that reflect processes at the regional to global scale. Changes in macro- and microfacies appear to mainly be related to changes in sea level and variations at several frequencies (or, orders) are recorded. Overall, the perceived sea-level changes throughout the succession at Kinnekulle agree well with those inferred from various proxies throughout Baltoscandia.

Acknowledgments

This study was funded by the Royal Physiographic Society in Lund (A.L.) and the Swedish Research Council (grant no. 2015-05084 to M.E.E). John Ahlgren, Peter Cederström and Anna Pettersson are thanked for assistance during fieldwork. Anna Pettersson is further thanked for help with map data. The workers at the Såtaskogen and Thorsberg quarries are thanked for their hospitality. Per Ahlberg and Stig Bergström are thanked for helpful discussions throughout the project. Christian Rasmussen is thanked for constructive comments on an earlier draft of this manuscript. Risto Kumpulainen, Brian Pratt and an anonymous reviewer are thanked for constructive comments that improved the final manuscript. This paper is a contribution to IGCP project 653 – 'The onset of the Great Ordovician Biodiversification Event'.

References

Adams, A.E., Mackenzie, W.S. & Guilford, C., 1984. *Atlas of sedimentary rocks under the microscope*. Longman Scientific and Technical, Essex. 104 pp.

Ainsaar, L., Meidla, T., Tinn, O., Martma, T. & Dronov, A., 2007: Darriwilian (Middle Ordovician) carbon isotope stratigraphy in Baltoscandia. *Acta Palaeontologica Sinica 46*, S1–S8.

Ainsaar, L., Kaljo, D., Martma, T., Meidla, T., Männik, P., Nõlvak, J. & Tinn, O. 2010: Middle and Upper Ordovician carbon isotope chemostratigraphy in Baltoscandia: a correlation standard and clues to environmental history. *Palaeogeography, Palaeoclimatology, Palaeoecology 294*, 189–201.

Albanesi, G.L., Bergström, S.M., Schmitz, B., Serra, F., Feltes, N.A., Voldman, G.G. & Ortega, G., 2013: Darriwilian (Middle Ordovician) $\delta^{13}C_{carb}$ chemostratigraphy in the Precordillera of Argentina: Documentation of the middle Darriwilian Isotope Carbon Excursion (MDICE) and its use for intercontinental correlation. *Palaeogeography, Palaeoclimatology, Palaeoecology 389*, 48–63.

Algeo, T. J., Marenco, P. J., Saltzman, M. R., 2016. Co-evolution of oceans, climate, and the biosphere during the 'Ordovician Revolution': A review. *Palaeogeography, Palaeoclimatology, Palaeoecology 458*, 1–11.

Bathurst, R.G.C., 1987: Diagenetically enhanced bedding in argillaceous platform limestones: stratified cementation and selective compaction. *Sedimentology 34*, 749–778.

Bergström, S.M. & Bergström, J., 1996: The Ordovician–Silurian boundary succession in Östergötland and Västergötland, S. Sweden. *GFF 118*, 25–42.

Bergström, S.M. & Löfgren, A., 2009: The base of the global Dapingian Stage (Ordovician) in Baltoscandia: conodonts, graptolites and unconformities. *Earth and Environmental Science Transactions of the Royal Society of Edinburgh 99 (for 2008)*, 189–212.

Bergström, S.M., Chen, X., Gutiérrez-Marco, J.C. & Dronov, A., 2009: The new chronostratigraphic classification of the Ordovician System and its relations to major regional series and stages and to $\delta^{13}C$ chemostratigraphy. *Lethaia 42*, 97–107.

Bergström, S.M., Eriksson, M.E., Young, S.A., Ahlberg, P. & Schmitz, B., 2014: Hirnantian (latest Ordovician) $\delta^{13}C$ chemostratigraphy in southern Sweden and globally: a refined integration with the graptolite and conodont zone successions. *GFF 136*, 355–386.

Bohlin, B., 1949: The Asaphus Limestone in northernmost Öland. *Bulletin of the Geological Institutions of the University of Uppsala 33*, 529–570.

Brett, C.E. & Baird, G., 1986: Comparative taphonomy: A key to paleoenvironmental interpretation based on fossil preservation. *Palaios 1*, 207–227.

Chen, J. & Lindström, M., 1991: Cephalopod Septal Strength Indices (SSI) and the depositional depth of Swedish Orthoceratite limestone. *Geologica et Palaeontologica 25*, 5–18.

De Geer, G., 1941: Om ortovarv, ett slags aglacial varvighet inom ortocerkalken. *Arkiv för Kemi, Mineralogi och Geologi 15*, 1–9.

Dronov, A.V. (ed.), 1997: Russian and International Bryozoan Conference, Bryozoa of the world: A field excursion guide, 30 June–8 July 1997, St. Petersburg. *Terra Nostra, Schriften der Alfred-Wegener-Stiftung 97/12*, 1–56.

Dronov, A.V., Ainsaar, L., Kaljo, D., Meidla, T., Saadre, T. and Einasto, R., 2011: Ordovician of Baltoscandia: Facies, sequences and sea-level changes. *In* J.C. Gutiérrez-Marco, I. Rábano, D. Garcia-Bellido (eds.): *Publicaciones del Instituto Geológico y Minero de España, Cuadernos del Museo Geominero 14: Ordovician of the world*. Instituto Geológico y Minero de España, Madrid, 143–150.

Dunham, R.J., 1962: Classification of carbonate rocks according to depositional texture. *In* W.E. Ham (ed.): Classification of Carbonate Rocks – A Symposium. *American Association of Petroleum Geologists Memoir 1*, 108–121.

Dzik, J. & Pisera, A., 1994: Sedimentation and fossils and Mójcza Limestone. *In* J. Dzik, E. Olempska & A. Pisera (eds.): Ordovician carbonate platform ecosystems of the Holy Cross Mountains. *Palaeontologica Polonica 53*, 5–41.

Eriksson, M.E., Lindskog, A., Calner, M., Mellgren, J.I.S., Bergström, S.M., Terfelt, F. & Schmitz, B., 2012: Biotic dynamics and carbonate microfacies of the conspicuous Darriwilian (Middle Ordovician) 'Täljsten' interval, south-central Sweden. *Palaeogeography, Palaeoclimatology, Palaeoecology 367–368*, 89–103.

Eriksson, M.E., Lindskog, A., Servais, T., Hints, O. & Tonarová, P., 2016: Darriwilian (Middle Ordovician) worms of southern Sweden. *GFF 138*, 502–509.

Fedorov, P.V., 2003: Lower Ordovician mud mounds from the St. Petersburg region, northwestern Russia. *Bulletin of the Geological Society of Denmark 50*, 125–137.

Flügel, E., 2010: *Microfacies of carbonate rocks: Analysis, interpretation and application*. Springer Verlag, Berlin. 984 pp.

Gillberg, G., 1970: Glacial geology of Kinnekulle, W. Sweden. *GFF 92*, pp. 347–381.

Gradstein, F.M., Ogg, J.G., Schmitz, M.D. & Ogg, G.M. (eds.), 2012: *The geologic time scale 2012*. Elsevier, Oxford. 1176 pp.

Hadding, A., 1958: The pre-Quaternary sedimentary rocks of Sweden. VII. Cambrian and Ordovician limestones. *Lunds Universitets Årsskrift, Ny Följd Afdelning 2, 54*, 1–261.

Haq, B.U. & Schutter, S.R., 2008: A chronology of Paleozoic sea-level changes. *Science 322*, 64–68.

Hessland, I., 1949. Investigations of the Lower Ordovician of the Siljan District, Sweden IV. Lithogenesis and changes of level in the Siljan District during a period of the Lower Ordovician – with a special discussion on the formation of chamositic ooids. *Bulletin of the Geological Institutions of the University of Uppsala 33*, 439–510.

Hilgen, F.J., Hinnov, L.A., Aziz, H.A., Abels, H.A., Batenburg, S., Bosmans, J.H.C., de Boer, B., Hüsing, S.K., Kuiper, K.F., Lourens, L.J., Rivera, T., Tuenter, E., van de Wal, Roderik, S.W., Wotzlaw, J.-F. & Zeeden, C., 2015: Stratigraphic continuity and fragmentary sedimentation: the success of cyclostratigraphy as part of integrated stratigraphy. *In* D.G. Smith, R.J. Bailey, P.M. Burgess & A.J. Fraser (eds.): Strata and time: probing the gaps in our understanding. *Geological Society, London, Special Publications 404*, 157–197.

Hints, O., Viira, V. & Nõlvak, J., 2012: Darriwilian (Middle Ordovician) conodont biostratigraphy in NW Estonia. Estonian. *Journal of Earth Sciences 61*, 210–226.

Hisinger, W., 1828. *Anteckningar i physik och geognosi under resor uti Sverige och Norrige, Fjerde häftet*. Elméns och Granbergs tryckeri, Stockholm. 260 pp.

Holm, G., 1901: I. Kinnekulles berggrund. *In* G. Holm & H. Munthe (eds.): Kinnekulle: Dess geologi och den tekniska användningen af dess bergarter. *Sveriges Geologiska Undersökning C172*, 1–76.

Holm, G. & Munthe, H. (eds.), 1901: Kinnekulle: Dess geologi och den tekniska användningen af dess bergarter. *Sveriges Geologiska Undersökning C172*, 1–144.
Holmer, L., 1983: Lower Viruan discontinuity surfaces in central Sweden. *GFF 105*, 29–42.
Högbom, A.G. & Ahlström, N.G., 1924: Über die subkambrische Landfläche am Fusse vom Kinnekulle. *Bulletin of the Geological Institutions of Uppsala 19*, 55–88.
Jaanusson, V., 1952: Untersuchungen über die Korngrösse der ordovizischen Kalksteine. *Geologiska Föreningens i Stockholm Förhandlingar 74*, 121–130.
Jaanusson, V., 1960: The Viruan (Middle Ordovician) of Öland. *Bulletin of the Geological Institutions of the University of Uppsala 38*, 207–288.
Jaanusson, V., 1964: The Viruan (Middle Ordovician) of Kinnekulle and Northern Billingen, Västergötland. *Bulletin of the Geological Institutions of the University of Uppsala 43*, 1–73.
Jaanusson, V, 1972: Constituent analysis of an Ordovician limestone from Sweden. *Lethaia 5*, 217–237.
Jaanusson, V., 1973: Aspects of carbonate sedimentation in the Ordovician of Baltoscandia. *Lethaia 6*, 11–34.
Jaanusson, V., 1976. Faunal dynamics in the Middle Ordovician (Viruan) of Balto-Scandia. *In* M.G. Bassett (ed.): *The Ordovician System: Proceedings of a Palaeontological Association symposium, Birmingham, September 1974*, 301–326. University of Wales Press and National Museum of Wales, Cardiff.
Jaanusson, V., 1982a: The Ordovician of Sweden. *In* D.L. Bruton & S.H. Williams (eds.): Field Excursion Guide. 4th International Symposium on the Ordovician System. *Paleontological Contributions from the University of Oslo 279*, 1–9.
Jaanusson, V., 1982b: Ordovician in Västergötland. *In* D.L. Bruton & S.H. Williams (eds.): Field Excursion Guide. 4th International Symposium on the Ordovician System. *Paleontological Contributions from the University of Oslo 279*, 164–183.
Jaanusson, V., 1982c: The Siljan district. *In* D.L. Bruton & S.H. Williams (eds.): Field Excursion Guide. 4th International Symposium on the Ordovician System. *Paleontological Contributions from the University of Oslo 279*, 15–42.
Jaanusson, V. & Mutvei, H., 1982. *Ordovician of Öland. Guide to excursion 3. IV International Symposium on the Ordovician System, Oslo 1982*. Swedish Museum of Natural History, Stockholm. 23 pp.
Johansson, B.S., Sundius, N. & Westergård, A.H. (eds.), 1943: Beskrivning till kartbladet Lidköping. *Sveriges Geologiska Undersökning Aa182*, 1–197.
Karis, L., 1998: Jämtlands östliga fjällberggrund. *In* L. Karis & A.G.B. Strömberg (eds.): Beskrivning till berggrundskartan över Jämtlands län, Del 2: Fjälldelen. *Sveriges Geologiska Undersökning Ca53:2*, 1–184.
Knaust, D. & Bromley, R.G. (eds.) 2012: Trace fossils as indicators of sedimentary environments. *Developments in Sedimentology 64*, 1–924.
Knaust., D. & Dronov, A., 2013: *Balanoglossites* ichnofabrics from the Middle Ordovician Volkhov Formation (St. Petersburg Region, Russia). *Stratigraphy and Geological Correlation 21*, 265–279.
Kröger, B. & Rasmussen, J.A., 2014: Middle Ordovician cephalopod biofacies and palaeoenvironments of Baltoscandia. *Lethaia 47*, 275–295.
Kumpulainen, R.A. (ed.), 2017: Guide for geological nomenclature in Sweden. *GFF 139*, 3–20.
Larsson, K., 1973: The lower Viruan in the autochthonous Ordovician sequence of Jämtland. *Sveriges Geologiska Undersökning C683*, 1–82.
Lindskog, A., 2014: Palaeoenvironmental significance of cool-water microbialites in the Darriwilian (Middle Ordovician) of Sweden. *Lethaia 47*, 187–204.
Lindskog, A., Eriksson, M.E. & Pettersson, A.M.L., 2014: The Volkhov–Kunda transition and the base of the Holen Limestone at Kinnekulle, Västergötland, Sweden. *GFF 136*, 167–171.
Lindskog, A., Eriksson, M.E., Tell, C., Terfelt, F., Martin, E., Ahlberg, P., Schmitz, B. & Marone, F., 2015: Mollusk maxima and marine events in the Middle Ordovician of Baltoscandia. *Palaeogeography, Palaeoclimatology, Palaeoecology 440*, 53–65.
Lindskog, A., Costa, M.M., Rasmussen, C.M.Ø., Connelly, J.N. & Eriksson, M.E., 2017: Refined Ordovician timescale reveals no link between asteroid breakup and biodiversification. *Nature Communications 8*, 14066 (doi: 10.1038/ncomms14066).

Lindström, M., 1963: Sedimentary folds and the development of limestone in an Early Ordovician sea. *Sedimentology 2*, 243–275.
Lindström, M., 1971a: Vom Anfang, Hochstand und Ende eines Epikontinentalmeeres. *Geologische Rundschau 60*, 419–438.
Lindström, M. 1971b: Small-scale domes and piercing-structures in the lower Ordovician limestones of Oeland (S.E. Sweden); comment on a paper by W. A. van Wamel. *Proceedings of the Koninklijke Nederlandse Akademie van Wetenschappen, Series B: Palaeontology, Geology, Physics and Chemistry 74*, 93–95.
Lindström, M., 1979: Diagenesis of Lower Ordovician hardgrounds in Sweden. *Geologica et Palaeontologica 13*, 9–30.
Lindström, M. & Vortisch, W., 1983: Indications of upwelling in the Lower Ordovician of Scandinavia. *In* J. Thiede & E. Suess (eds.): *Coastal upwelling*, 535–551. Plenum, New York.
Linnarsson, J.G.O., 1866: *Om de siluriska bildningarne i mellersta Westergötland I*. Akademisk afhandling, Filosofiska fakulteten i Uppsala. 23 pp.
Linnarsson, J.G.O., 1869: Om Vestergötlands cambriska och siluriska aflagringar. *Kungliga Svenska Vetenskaps-Akademiens Handlingar 8*, 1–89.
Löfgren, A., 1995: The middle Lanna/Volkhov Stage (middle Arenig) of Sweden and its conodont fauna. *Geological Magazine 132*, 693–711.
Meidla, T., Ainsaar, L. & Hints, O., 2014: The Ordovician System in Estonia. *In* H. Bauert, O. Hints, T. Meidla & P. Männik (eds.): *4th Annual Meeting of IGCP 591, Estonia, 10–19 June 2014. Abstracts and Field Guide*, 116–122. University of Tartu, Tartu.
Mellgren, J.I.S. & Eriksson, M.E., 2010: Untangling a Darriwilian (Middle Ordovician) palaeoecological event in Baltoscandia: conodont faunal changes across the 'Täljsten' interval. Earth and Environmental Science Transactions of the Royal Society of Edinburgh 100, 353–370.
Moberg, J.C., 1910: Historical-stratigraphical review of the Silurian of Sweden. *Sveriges Geologiska Undersökning C229*, 1–210.
Munthe, H., 1905: De geologiska hufvuddragen af Västgötabergen och deras omgifning. *Geologiska Föreningens i Stockholm Förhandlingar 27*, 347–401.
Männil, R.M. (Мяннль, Р.М.), 1966: *История развития Балтийского бассейна в ордовике* [*Evolution of the Baltic Basin during the Ordovician*]. Eesti NSV Teaduste Akadeemia Geoloogia Institut, Tallinn. 199 pp.
Nielsen, A.T., 1995: Trilobite systematics, biostratigraphy and palaeoecology of the Lower Ordovician Komstad Limestone and Huk formations, southern Scandinavia. *Fossils and Strata 38,* 1–374.
Nielsen, A.T., 2004: Ordovician sea level changes: a Baltoscandian perspective. *In* B.D. Webby, F. Paris, M.L. Droser & I.G. Percival (eds.): *The Great Ordovician Biodiversification Event*, 84–93. Columbia University Press, New York.
Nielsen, A.T., 2011: A re-calibrated revised sea-level curve for the Ordovician of Baltoscandia. *In* J.C. Gutiérrez-Marco, I. Rábano, D. Garcia-Bellido (eds.): *Publicaciones del Instituto Geológico y Minero de España, Cuadernos del Museo Geominero 14: Ordovician of the world*. Instituto Geológico y Minero de España, Madrid, 399–401.
Nielsen, A.T. & Schovsbo, N.H., 2015: The regressive Early–Mid Cambrian 'Hawke Bay Event' in Baltoscandia: Epeirogenic uplift in concert with eustasy. *Earth-Science Revews 151*, 288–350.
Nordlund, U., 1989: Lithostratigraphy and sedimentology of a Lower Ordovician limestone sequence at Hälludden, Öland, Sweden. *GFF 111*, 65–94.
Olgun, O. 1987. Komponenten-Analyse und Conodonten-Stratigraphie der Orthoceratenkalksteine im Gebiet Falbygden, Västergötland, Mittelschweden. *Sveriges Geologiska Undersökning Ca70*, 1–78.
Paul, C.R.C. & Bockelie, J.F., 1983: Evolution and functional morphology of the cystoid Sphaeronites in Britain and Scandinavia. *Palaeontology 26*, 687–734.
Pohl, A., Donnadieu, Y., Le Hir, G., Ladant, J.-B., Dumas, C., Alvarez-Solas, J. & Vandenbroucke, T.R.A., 2016: Glacial onset predated Late Ordovician climate cooling. *Paleoceanography 31*, 800–821.

Põlma, L. [Пылма, Л.], 1982: *Сравнительная литология карбонатных пород ордовика Северной и Средней Прибалтики* [*Comparetive lithology of Ordovician carbonate rocks in North and Central East Baltic*]. Valgus, Tallinn. 152 pp.

Priem, H.N.A., Mulder, F.G., Boelrijk, N.A.I.M., Hebeda, E.H., Verschure, R.H. & Verdurmen, E.A.T., 1968: Geochronological and palaeomagnetic reconnaissance survey in parts of central and southern Sweden. *Physics of the Earth and Planetary Interiors 1*, 373–380.

Rasmussen, C.M.Ø., Nielsen, A.T. & Harper, D.A.T., 2009: Ecostratigraphical interpretation of lower Middle Ordovician East Baltic sections based on brachiopods. *Geological Magazine 146*, 717–731.

Rasmussen, C.M.Ø., Ullmann, C.V., Jakobsen, K.G., Lindskog, A., Hansen, J., Hansen, T., Eriksson, M.E., Dronov, A., Frei, R., Korte, C., Nielsen, A.T. & Harper, D.A.T., 2016: Onset of main Phanerozoic marine radiation sparked by emerging Mid Ordovician icehouse. *Scientific Reports 6*, 18884 (doi: 10.1038/srep18884).

Rasmussen, J.A. & Stouge, S., 1995: Late Arenig–early Llanvirn conodont biofacies across the Iapetus Ocean. *In* J.D. Cooper, M.L. Droser & S.C. Finney (eds.): *Ordovician Odyssey: Short Papers for the Seventh International Symposium on the Ordovician System*. *SEPM, Pacific Section 77*, 443–447.

Rasmussen, J.A., Bruton, D.L. & Nakrem, H.A., 2013: Stop 17. Tremadocian to Darriwilian units, Bjørkåsholmen and Djuptrekkodden, Slemmestad. *In* M. Calner, P. Ahlberg, O. Lehnert & M. Erlström (eds.): The Lower Palaeozoic of Southern Sweden and the Oslo Region, Norway. Field guide for the 3rd annual meeting of the IGCP project 591. *Sveriges Geologiska Undersökning Rapporter och meddelanden 133*, 67–72.

Regnéll, G., 1945: Non-crinoid Pelmatozoa from the Paleozoic of Sweden: *Meddelanden från Lunds Geologisk-Mineralogiska Institution 108*, 1–255.

Regnéll, G., 1948: An outline of the succession and migration of non-crinoid pelmatozoan faunas in the Lower Paleozoic of Scandinavia. *Arkiv för Kemi, Mineralogi och Geologi 26A:13*, 1–55.

Reyment, R.A., 1970: Vertically inbedded cephalopod shells. Some factors in the distribution of fossil cephalopods, 2. *Palaeogeography, Palaeoclimatology, Palaeoecology 7*, 103–111.

Rutten, M.G., 1949: Actualism in epeirogenetic oceans. *Geologie en Mijnbouw*. 11, 222–228.

Saadre, T., Einasto, R., Nõlvak, J. & Stouge, S., 2004: Ordovician stratigraphy of the Kovel-1 well (Volkhov–Haljala) in the Volynia region, northwestern Ukraine. *Bulletin of the Geological Society of Denmark 51*, 47–69.

Schieber, J., Southard, J.B., Kissling, P., Rossman, B. & Ginsburg, R., 2013: Experimental deposition of carbonate mud from moving suspensions: importance of flocculation and implications for modern and ancient carbonate mud deposition. *Journal of Sedimentary Research 83*, 1025–1031.

Schlager, W., 2005: Carbonate sedimentology and sequence stratigraphy. *SEPM Concepts in Sedimentology and Paleontology 8*, 1–206.

Schmitz, B., 2013. Extraterrestrial spinels and the astronomical perspective on Earth's geological record and evolution of life. *Chemie der Erde – Geochemistry 73*, 117–145.

Schmitz, B., Bergström, S.M. & Xiaofeng, W., 2010: The middle Darriwilian (Ordovician) $\delta^{13}C$ excursion (MDICE) discovered in the Yangtze Platform succession in China: implications of its first recorded occurrences outside Baltoscandia. *Journal of the Geological Society 167*, 249–259.

Servais, T., Harper, D.A.T., Li, J., Munnecke, A., Owen, A.W., Sheehan, P.M., 2009. Understanding the Great Ordovician Biodiversification Event (GOBE): Influences of paleogeography, paleoclimate, or paleoecology? *GSA Today 19*, 4–10.

Stephansson, O., 1971: Gravity tectonics on Öland. *Bulletin of the Geological Institutions of the University of Uppsala, New Series, 3*, 37–78.

Sturesson, U., 1989: Coated grains in Lower Viruan limestones in Västergötland, central Sweden. *GFF 111*, 273–284.

Thorslund, P., 1958, Djupborrningen på Gotska Sandön. *Geologiska Föreningens i Stockholm Förhandlingar 80*, 190–197.

Thorslund, P. & Westergård, A.H., 1938: Deep boring through the Cambro-Silurian at File Haidar, Gotland. *Sveriges Geologiska Undersökning C415*, 1–57.

Tinn, O. & Meidla, T., 2001: Middle Ordovician ostracods from the Lanna and Holen Limestones, south-central Sweden. *GFF 123*, 129–136.

Tjernvik, T., 1956: On the early Ordovician of Sweden. Stratigraphy and fauna. *Bulletin of the Geological Institutions of the University of Uppsala 36*, 107–284.

Tjernvik, T.E. & Johansson, J.V., 1979: Description of the upper portion of the drill-core from Finngrundet in the South Bothnian Bay. *Bulletin of the Geological Institutions of the University of Uppsala 8*, 113–204.

Trotter, J.A., Williams, I.S., Barnes, C.R., Lécuyer, C. & Nicoll, R.S., 2008: Did cooling oceans Trigger Ordovician biodiversification? Evidence from conodont thermometry. *Science 321*, 550–554.

Ulmer, P.A. & Ulmer-Scholle, D.S., 2006: A Color Guide to the Petrography of Carbonate Rocks: Grains, textures, porosity, diagenesis. *American Association of Petroleum Geologists Memoir 77*, 1–474.

van Wamel, W.A., 1970: Small-scale domes and piercing-structures in the Lower Ordovician limestones of Oeland (S.E. Sweden). *Proceedings of the Koninklijke Nederlandse Akademie van Wetenschappen, Series B: Palaeontology, Geology, Physics and Chemistry 73*, 293–304.

Webby, B.D., Paris, F., Droser, M.L. & Percival, I.G. (eds.), 2004: *The Great Ordovician Biodiversification Event*. Columbia University Press, New York. 484 pp.

Westergård, A.H., 1928: Den kambro-siluriska lagerserien. *In* H. Munthe, A.H. Westergård & G. Lundqvist (eds.): Beskrivning till kartbladet Skövde. *Sveriges Geologiska Undersökning Aa121*, 21–64.

Westergård, A.H., 1943: Den kambro-siluriska lagerserien. *In* S. Johansson, N. Sundius & A.H. Westergård (eds.): Beskrivning till kartbladet Lidköping. *Sveriges Geologiska Undersökning Aa182*, 22–89.

Wu, R., Stouge, S., Percival, I.G. & Zhan, R., 2014: Early–Middle Ordovician conodont biofacies on the Yangtze Platform margin, South China: Applications to palaeoenvironment and sea-level changes. *Journal of Asian Earth Sciences 96*, 194–204.

Wu, R., Calner, M. & Lehnert, O., in press: Integrated conodont biostratigraphy and carbon isotope chemostratigraphy in the Lower–Middle Ordovician of southern Sweden reveals a complete record of the MDICE. *Geological Magazine*

Wærn, B., Thorslund, P. & Henningsmoen, G., 1948: Deep boring through Ordovician and Silurian strata at Kinnekulle, Vestergötland. *Bulletin of the Geological Institutions of the University of Uppsala 32*, 337–474.

Zhang, J., 1998a: Middle Ordovician conodonts from the Atlantic Faunal Region and the evolution of key conodont genera. *Meddelanden från Stockholms universitets institution för geologi och geokemi 298*, 27 pp.

Zhang J., 1998b: The Ordovician conodont genus *Pygodus*. In H. Szaniawski (ed.): Proceedings of the Sixth European Conodont Symposium (ECOS VI). *Palaeontologia Polonica 58*, 87–105.

Zhang, Y. & Munnecke, A., 2016: Ordovician stable carbon isotope stratigraphy in the Tarim Basin, NW China. *Palaeogeography, Palaeoclimatology, Palaeoecology 458*, 154–175.

FIGURES

Fig. 1. Map of southern Sweden and the surrounding Baltoscandian region. Geographic areas (e.g., localities, provinces) discussed in the main text are indicated. The distribution of lower Paleozoic rocks is indicated by green shading; areas with significant outcrops of Ordovician strata are indicated by darker shading (after Jaanusson 1982b; Lindskog 2014; Nielsen & Schovsbo 2015).

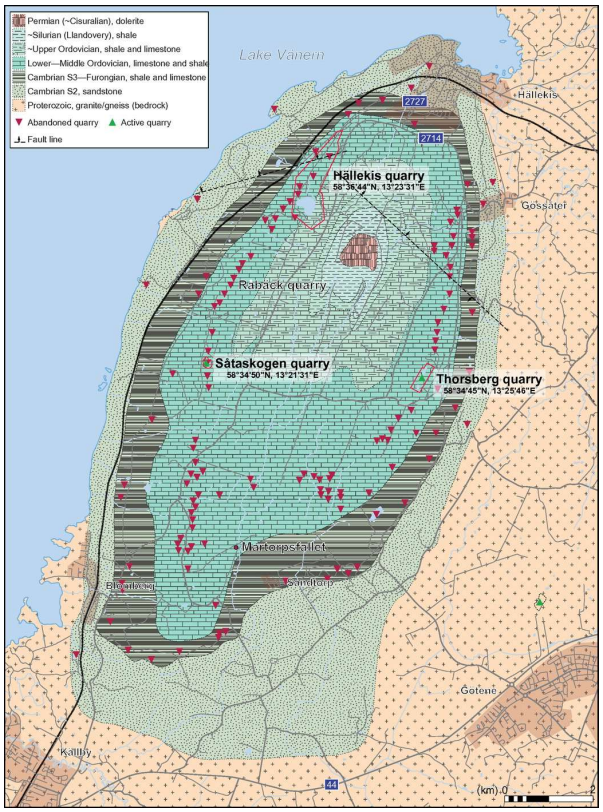

Fig. 2. Map of the Kinnekulle area, with main lithologies indicated (after Johansson et al. 1943). A string of abandoned quarries in the Middle Ordovician limestone area trace the outcropping of the 'orthoceratite limestone', in particular the 'Täljsten' and enclosing beds.
GPS coordinates are given according to the WGS 84 reference system.

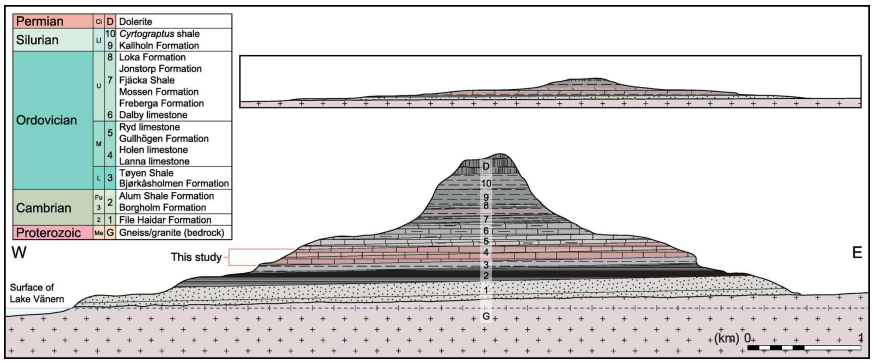

Fig. 3. Diagrammatic profile of Kinnekulle, as viewed from west to east, with distinct lithologic intervals indicated (vertical scale enhanced five times). The inset figure shows the same profile with vertical axis to scale. Modified from Johansson et al. (1943), with modernized stratigraphic subdivision after Wærn et al. (1948), Jaanusson (1964, 1982a, b), Priem et al. (1968), Bergström and Bergström (1996) Bergström et al. (2014) and Lindskog et al. (2014).

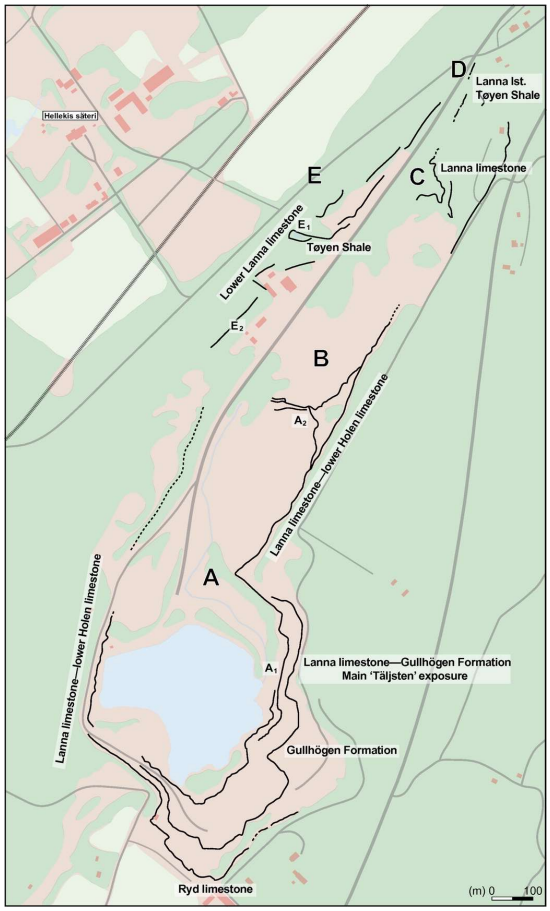

Fig. 4. Sketch map of the Hällekis quarry, with subsections (A–E) and points of interest (see main text) indicated. Heavy black lines indicate accessible rock outcrops.

Fig. 5. Photographs of the Hällekis quarry. **A.** The southernmost part of the Hällekis quarry, southern Hällekis A (A_1, main) section, with the exposed (topo-)formations indicated (view towards the east). **B.** Northern end of Hällekis A (view towards the southeast). Note the gray ‘Täljsten’ beds (c. 1 m) in the upper part for scale. **C.** Fault/fold structure in the northernmost end of Hällekis A (A_2; view towards the east). Stippled lines indicate traceable horizons, highlighting displacements during warping of the strata. The figured succession is c. 8 m thick. **D.** Hällekis B, which follows to the north of the fold structure in Hällekis A (view towards the northeast). The strata have been displaced c. 5 m downwards. **E.** Hällekis C (view towards the east). The rock wall is c. 10 m high. **F.** Hällekis D (view towards the east). Boundary between the Tøyen Shale and the Lanna limestone indicated by arrow. **G.** A typical outcrop along Hällekis E (view towards the northwest).

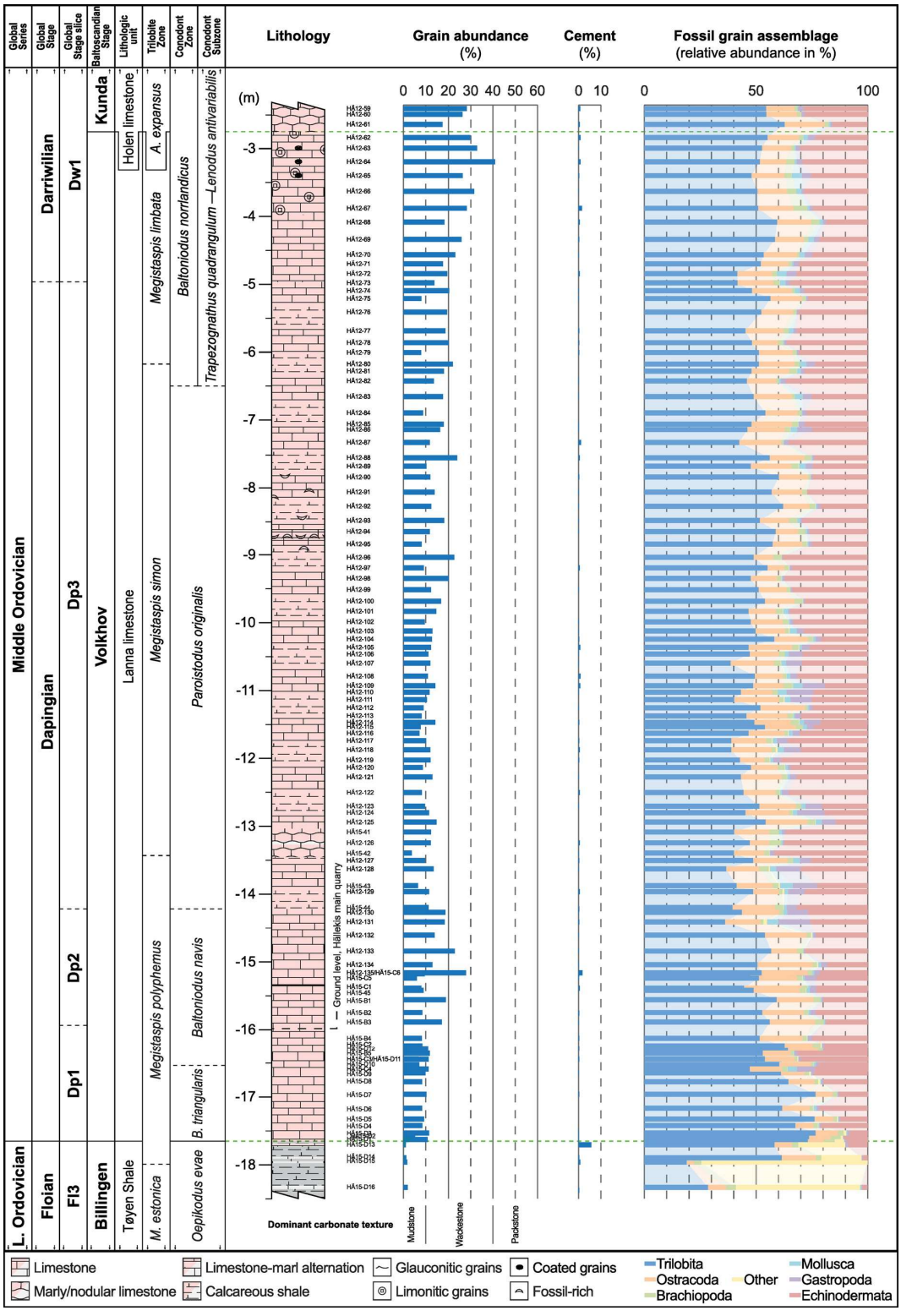

Fig. 6. Sedimentary profile of the uppermost Tøyen Shale and Lanna limestone at the Hällekis quarry, northwestern Kinnekulle. Biostratigraphy after Tjernvik (1956), Zhang (1998a), Bergström & Löfgren (2009), Schmitz et al. (2010) and Lindskog et al. (2014, 2015), with middle part extrapolated from Nielsen (1995) and Löfgren (1995).

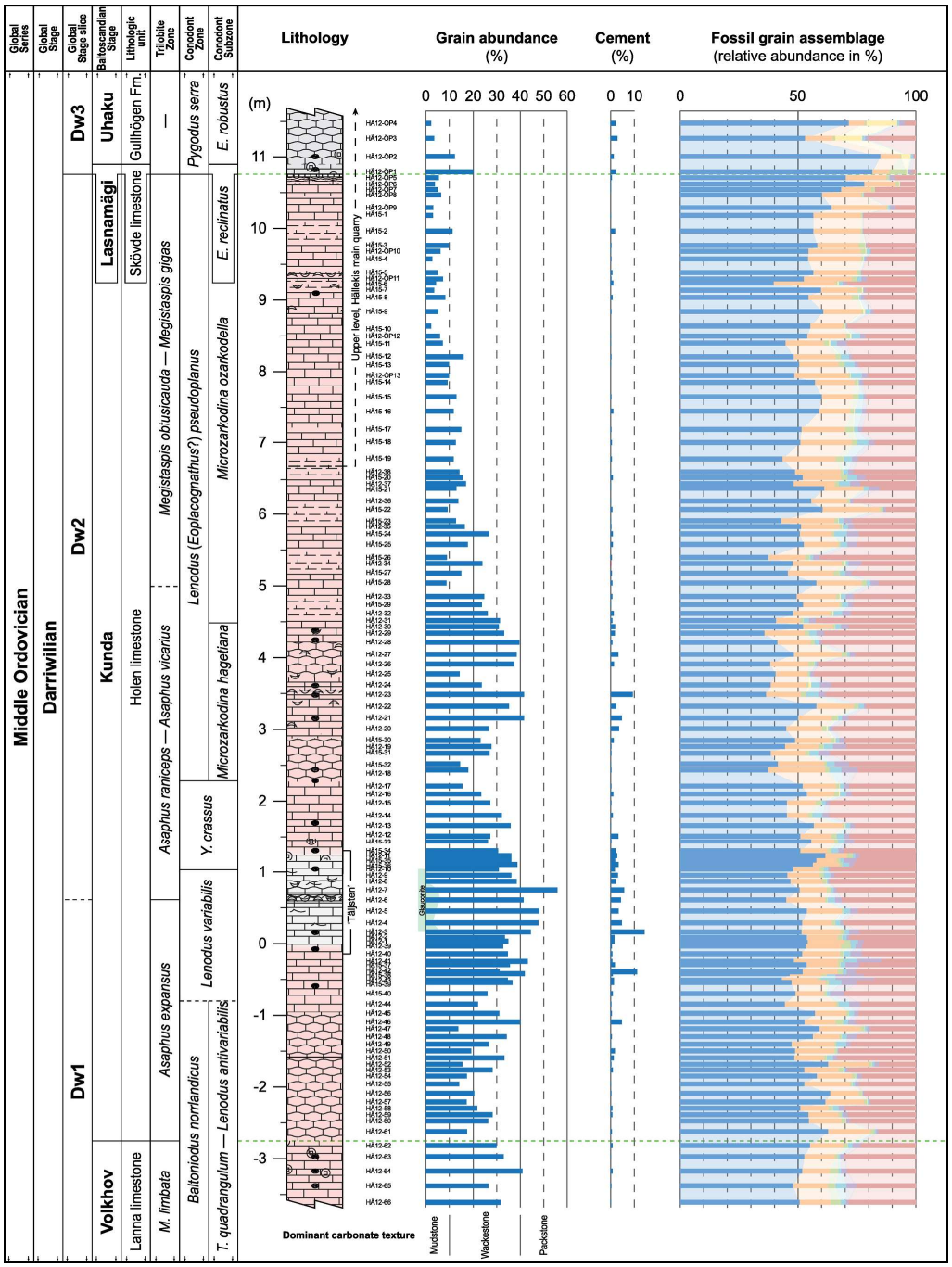

Fig. 7. Sedimentary profile of the Holen limestone, Skövde limestone and the lowermost Gullhögen Formation at the Hällekis quarry, northwestern Kinnekulle. Biostratigraphy after Zhang (1998a, b) and Lindskog (2014).

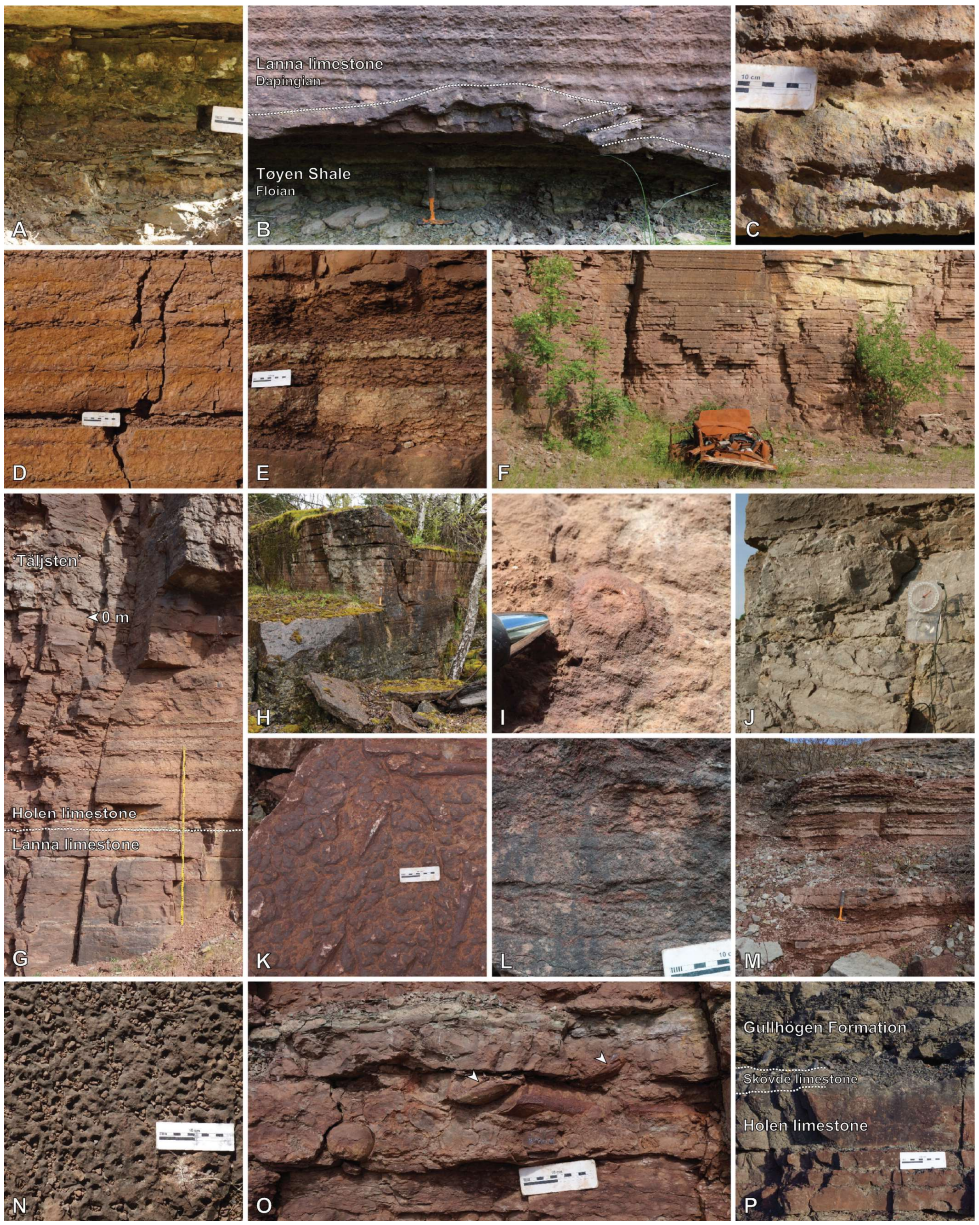

Fig. 8. Field photographs of characteristic lithologic and sedimentologic features. **A.** The uppermost Tøyen Shale (Hällekis D; main increments in scale 1 cm). The base of the Lanna limestone forms the roof overhang in the picture. **B.** The Tøyen Shale–Lanna limestone (~Floian–Dapingian) transition (Hällekis E_1). A dome-shaped structure has formed in the lowermost Lanna limestone (indicated by stippled line). Hammer (c. 30 cm long) for scale. **C.** Dense accumulation of heavily bioeroded limonite-stained hardgrounds in the basal Lanna limestone (Hällekis D). **D.** Bedding in the lower Lanna limestone (Hällekis C). Note the flat discontinuity surface and associated bioerosion beneath the scale. **E.** Marly and finely nodular interval in the lower Lanna limestone, which is traceable throughout most of the Hällekis quarry (Hällekis A). **F.** The middle Lanna limestone, characterized by relatively thin, competent limestone beds alternating with easily weathering marly interbeds (Hällekis C). Subfossil vehicle (Holocene, *Volvo 244* automobile Zone, AD 1974 and onwards) for scale. **G.** The Holen limestone–Lanna limestone (Volkhov–Kunda) boundary beds (Hällekis A). Reference (0 m) level used during stratigraphic measurements indicated by arrow. **H.** The 'Täljsten' and overlying beds (abandoned quarry, eastern Kinnekulle). **I.** Crinoid holdfast on an exposed bedding surface in the lowermost 'Täljsten' (Såtaskogen quarry). **J.** The 'Täljsten' (Hällekis A). **K.** Bedding surface with hematite-rich structures likely of microbial origin (c. 0.5 m below the 'Täljsten', Såtaskogen quarry). **L.** Interval with hematite-stained stromatolitic bedding (c. 0.3 m above 'Täljsten', abandoned quarry, western Kinnekulle; 58°35'40"N, 13°21'60"E). **M.** Limestone-marl alternation in the uppermost Holen limestone (Hällekis A). **N.** Numerous shallow circular borings/burrows in an exposed and slightly

weathered bedding surface in the upper Holen limestone (Hällekis A). **O.** Dense collection of coarse skeletal debris in the upper Holen limestone (Hällekis A). **P.** The Holen limestone (Kunda)–Skövde limestone (Lasnamägi)–Gullhögen Formation (Lasnamägi/Uhaku) transition (Hällekis A).

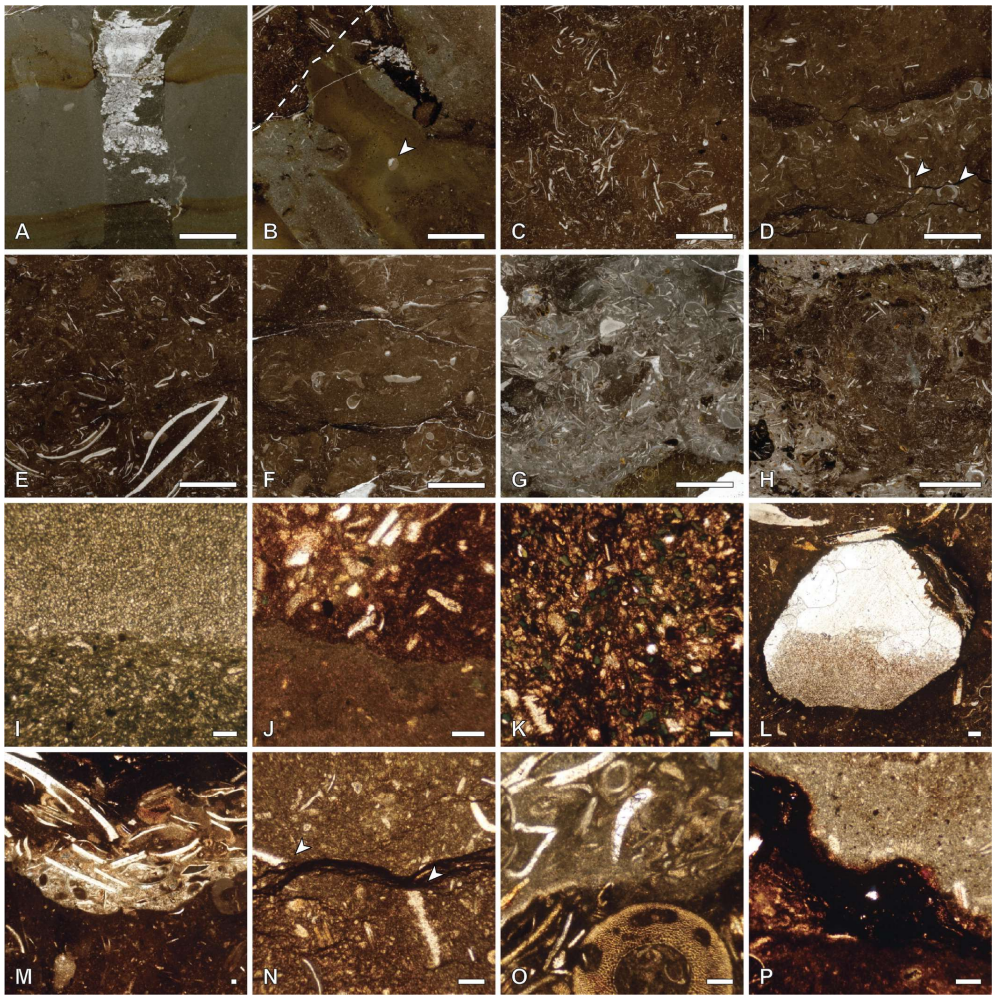

Fig. 9. Thin-section micrographs from the Tøyen Shale–Lanna limestone interval. Scale bars in A–H 5 mm (all images to same scale for straightforward comparison). Scale bars in I–P 100 µm (images variably scaled). **A.** Calcareous mudstone in the uppermost Tøyen Shale, with large vertical burrow in the center (HÄ15-D14; transmitted light). The light-colored material in the burrow is crystalline barite and calcite. **B.** Limonitic hardground with numerous macroborings (HÄ15-D2; transmitted light). The bedding (indicated by stippled line) has been deformed during diagenesis; arrow marks geopetal tube filling indicating original horizontality of the bedding. **C.** Wackestone in the lower Lanna limestone (HÄ12-133; transmitted light). **D.** Wackestone/mudstone in the lower-middle Lanna limestone with numerous dissolution seams filled with fine-grained siliciclastic matter (HÄ12-123; transmitted light). Several grains have been truncated during the dissolution (arrows). **E.** Wackestone with coarse skeletal grains (HÄ12-101; transmitted light). **F.** Mudstone/wackestone with numerous dissolution features (HÄ12-87; transmitted light). **G.** Wackestone–packstone bed in the upper Lanna limestone (HÄ12-67; transmitted light). A limonitic hardground surface occurs in the lower right. **H.** Coarse-textured bed in the upper Lanna limestone, strewn with limonitic grains and numerous intraclasts (HÄ12-64; transmitted light). **I.** Calcareous mudstone in the upper Tøyen Shale (HÄ15-D15; plane-polarized light). Diagenetic recrystallization has led to a coarsening of the matrix. Note the shift vertically between two distinct facies. **J.** Limonitic hardground in the basal Lanna limestone overlain by sediment strewn with trilobite fragments (HÄ15-D3; plane-polarized light). **K.** Burrow/boring filling in basal Lanna limestone hardground containing numerous glauconite grains and comminuted skeletal material (HÄ15-D1; plane-polarized light)**. L.** Tube-shaped horizontal boring/burrow below flat hardground in the lower Lanna limestone (HÄ15-C1; plane-polarized light; see also Fig. 8D). The

tube was originally left open and became partly filled with sediment that has been slightly recrystallized (similar to vadose silt; see Flügel, 2010). Coarse calcite filled the remaining void. **M.** Depression in mudstone/wackestone filled with coarse skeletal grains forming a thin horizon of grainstone and packstone (HÄ12-109; plane-polarized light). **N.** Close-up of clay-filled dissolution seam (HÄ12-77; plane-polarized light). Several grains have been truncated against it. **O.** Limonitic hardground in the upper Lanna limestone (HÄ12-67; plane-polarized light). **P.** Hematite-stained stromatolitic structure on a hardground surface (HÄ12-62; plane-polarized light).

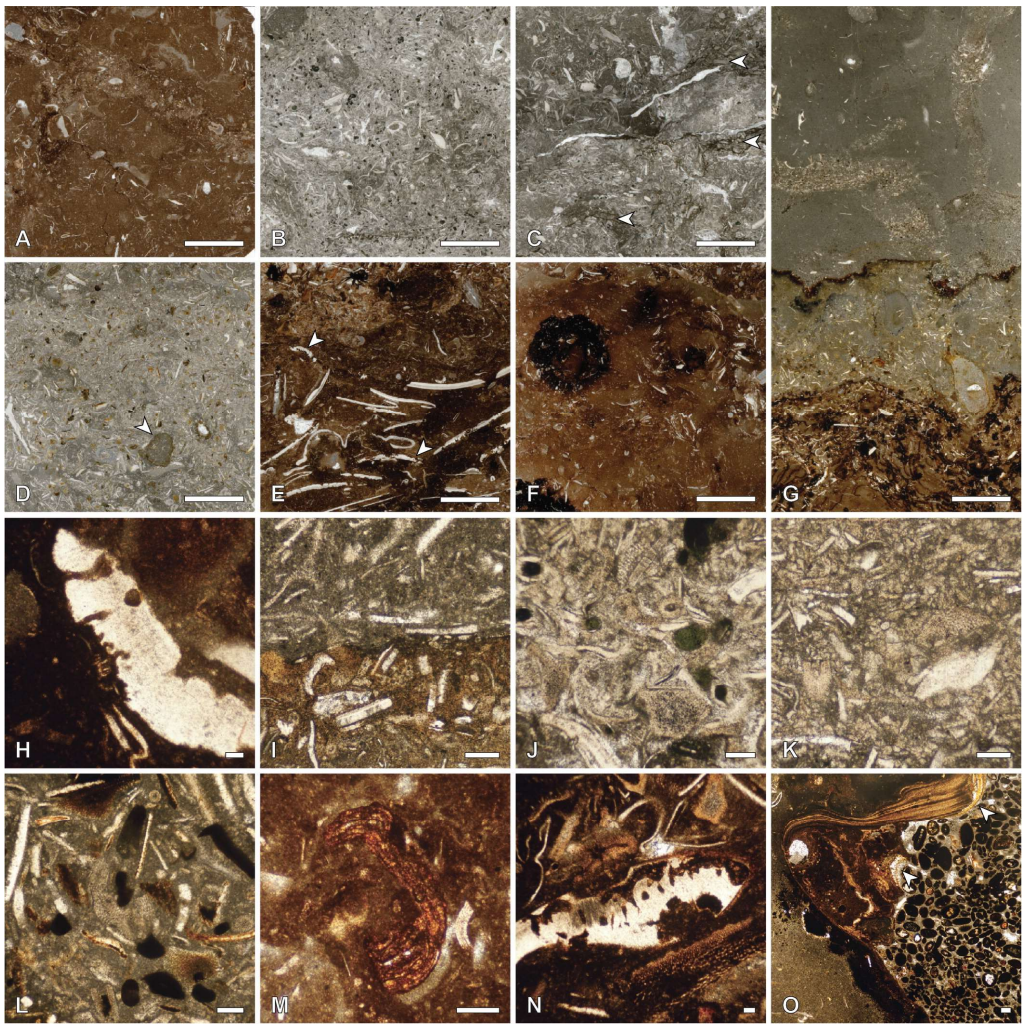

Fig. 10. Thin-section micrographs from the Holen limestone–Gullhögen Formation interval. Scale bars in A–G 5 mm (all images to same scale). Scale bars in H–P 100 µm (images variably scaled). **A.** Wackestone in the lowermost Holen limestone (HÄ12-57; transmitted light). **B.** Glauconitic packstone/wackestone in the lower 'Täljsten' (HÄ12-3; transmitted light). **C.** Packstone/wackestone in the middle 'Täljsten'. Dissolution seams (arrows) occur abundantly (HÄ12-6; transmitted light). **D.** Wackestone/packstone strewn with limonitic grains in the uppermost 'Täljsten' (HÄ12-11; transmitted light). **E.** Coarse skeletal material in the middle Holen limestone (HÄ12-20; transmitted light). Note abundant microborings in the grains (arrows indicate illustrative examples). **F.** Hematite-stained mudstone/wackestone in the upper Holen limestone (HÄ15-13; transmitted light). **G.** The boundary between the Holen limestone and the Skövde limestone, marked by the discontinuity surface in the middle (HÄ12-ÖP5/HÄ12-ÖP1; transmitted light). **H.** Trilobite fragment bored by endolithic microorganisms (HÄ12-53; plane-polarized light). See also N. **I.** Phosphatic hardground in the lower 'Täljsten' (HÄ12-2; plane-polarized light). **J.** Glauconitic packstone/grainstone in the lower 'Täljsten' (HÄ12-3; plane-polarized light). **K.** Finely comminuted skeletal grains in the lower-middle 'Täljsten' (HÄ12-4; plane-polarized light). **L.** Wackestone/packstone strewn with limonitic (brown to opaque) grains (HÄ15-36; plane-polarized light). **M.** Detached stromatolitic crust (HÄ12-24; plane-polarized

light). **N.** Trilobite grain with numerous endolithic microborings (HÄ12-26; plane-polarized light). **O.** Sedimentary filling within a depression in the flat discontinuity surface at the top of the Holen limestone (base of Skövde limestone; HÄ12-ÖP5; plane-polarized light). Numerous generations of sediment and cements are visible, including a laminated phosphatic crust in the roof and left walls of the original cavity, crystalline calcite (arrows), phosphatic mudstone (left) and oolitic packstone (right). The rim of the depression has been stained by ferruginous compounds.

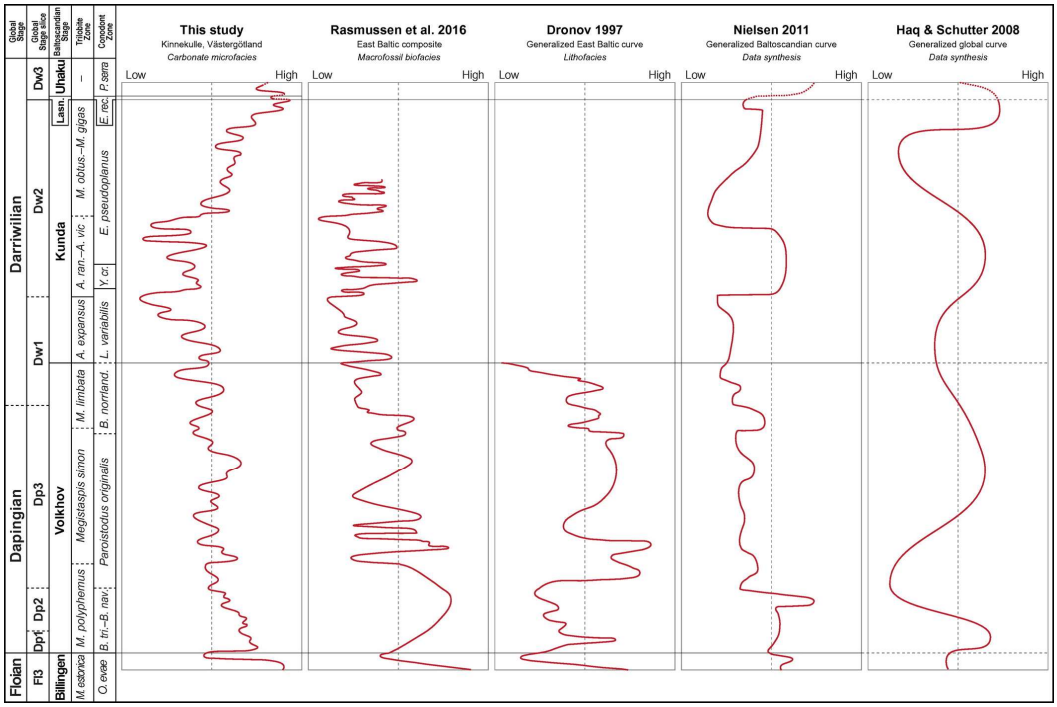

Fig. 11. Inferred sea level curve spanning the studied time interval, compared to previously published curves. The different curves are arranged in order of decreasing correlativity and resolution. All curves are scaled against the biostratigraphic scheme used herein.